

Award Accounts

The Chemical Society of Japan Award for Young Chemists for 2003

Synthetic Strategy for Rational Design of Single-Chain Magnets

Hitoshi Miyasaka*[,1,2] and Rodolphe Clérac*[,3]

[1]Department of Chemistry, Graduate School of Science, Tokyo Metropolitan University, 1-1 Minami-ohsawa, Hachioji, Tokyo 192-0397

[2]"Structural Ordering and Physical Properties," PRESTO, Japan Science and Technology Agency, 4-1-8 Honcho, Kawaguchi, Saitama 332-0012

[3]Centre de Recherche Paul Pascal, CNRS UPR 8641, 115 avenue du Dr. A. Schweitzer, 33600 Pessac, France

Received February 2, 2005; E-mail: miyasaka@comp.metro-u.ac.jp

A magnetically-isolated one-dimensional chain can behave as if "magnet"— this sentence may be opposed to our common sense. In this review, we will show that a "magnet-like" behavior can effectively be found in only a magnetic spin chain. In 2001, which is almost forty years after the pioneering theoretical work of R. J. Glauber [*J. Math. Phys.*, **4**, 294 (1963)] on the dynamics of ferromagnetically-coupled Ising spin chains, the first experimental evidence of such behavior has been discovered in a real one-dimensional compound [A. Caneschi et al. *Angew. Chem., Int. Ed.*, **40**, 1760 (2001)]. In 2002, we have reported on a one-dimensional compound $[Mn_2(saltmen)_2Ni(pao)_2(py)_2](ClO_4)_2$ ($saltmen^{2-}$ = *N*,*N*′-(1,1,2,2-tetramethylethylene)bis(salicylideneiminato), pao^- = pyridine-2-aldoximato, and py = pyridine) which can be considered as a chain of ferromagnetically-coupled anisotropic $S_T = 3$ units [*J. Am. Chem. Soc.*, **124**, 12837 (2002)]. Magnetic measurements on this compound revealed the presence of slow relaxation and large field-dependent hysteresis of the magnetization at low temperatures. The topology of this chain is very close to the "ideal" chain imagined by Glauber and hence, still to date, the simplest system to probe the Glauber dynamics. By analogy to the Single-Molecule Magnets described in the introduction of this paper, we called this type of material: Single-Chain Magnet (SCM). To obtain simple SCM systems, we have developed a step-by-step synthetic strategy using primary and secondary building blocks to control the chemistry of the targeting materials and the physics of their characteristic magnetic properties. In this review, we will describe this synthetic strategy from the elementary building blocks to the final series of Single-Chain Magnets obtained since 2002. The magnetic properties of all these materials will be discussed in detail. In particular, the experimental SCM behavior will be described and analyzed in relation with the generalization of the Glauber model for real systems.

The syntheses of Single-Molecule Magnet (SMM) and Single-Chain Magnet (SCM) are current challenges in the fields of molecule-based magnetism and solid-state physics.[1–5] While these systems set the academic community theoretical questions, their potential uses in devices for information storage at the molecular and nano-scale levels have given a strong impetus to this field.[6–11] After the discovery of the SMM behavior in the well-known Mn_{12} family,[12] many other SMM clusters have been prepared based on Mn,[13,14] Fe,[15] Ni,[16] V,[17] Co,[18] or mixed-metals[19,20] polynuclear complexes. Their characteristic magnetic properties and related physical phenomena have been widely investigated to understand the magnetization dynamics and the intrinsic quantum effects.[21–35] In these systems, the slow relaxation of the magnetization is induced by a combined effect of a high spin ground state (S_T), an uni-axial anisotropy (zero-field splitting parameter, D), and a small transverse anisotropy of the transition-metal-based complex. The former two characteristics create an energy barrier, Δ, between "spin-up" and "spin-down" configurations of the spin ground state ($m_s = \pm S_T$). From the energy diagram of the spin ground state which can be viewed as a double-well potential scheme (Fig. 1), this gap can be easily estimated at $|D|S_T^2$ for integer S_T spin and $|D|(S_T^2 - 1/4)$ for half-integer S_T spin.[4] When a magnetic field is applied on this system, the magnetization therefore saturates and consequently removes the ground state degeneracy. After the applied field is switched off, the magnetization decays with a single relaxation time, τ, to recover the thermodynamic equilibrium between the two m_s levels. Experimentally, τ follows an Arrhenius law, $\tau = \tau_0 \exp(\Delta/k_B T)$ (where τ_0 is the pre-exponential factor and k_B is the Boltzmann constant), with an activation energy equal to Δ. The exponential enhancement of the relaxation time with lowering temperature leads to a return at the equilibrium with a very long (relaxation) time, sometimes reaching several years. Hence, these materials display a large-field hysteresis of the magnetization at low temperatures and can be therefore

Published on the web October 4, 2005; DOI 10.1246/bcsj.78.1725

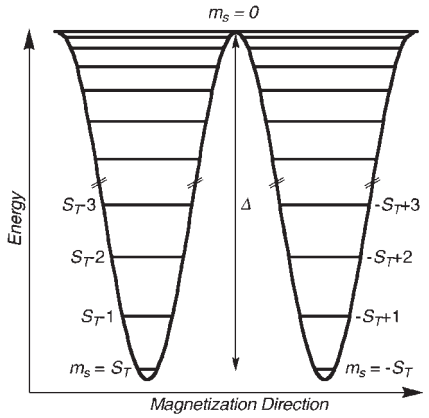

Fig. 1. Double-well potential energy scheme of the ground spin state, S_T, in SMMs (at $H_z = 0$).

considered as if "magnets."

In 1963, R. J. Glauber have reported that an infinite one-dimensional arrangement of ferromagnetically-coupled Ising spins could also experience slow relaxation of the magnetization.[36,37] In these one-dimensional systems, the "magnet-type" behavior is induced not only (i) by the uni-axial anisotropy (D) and the high spin ground state (S_T) of the repeating unit of chain (note that similar ingredients are used to describe the SMM behavior) but also (ii) by the correlation (J) operating along the chain. It is well-known that independently of the spin dimensionality, n ($n = 1$, Ising; $n = 2$, XY; $n = 3$, Heisenberg), one-dimensional systems do not experience long-range order at any finite temperature (at only $T = 0$ K).[38] Nevertheless, as for SMM, these one-dimensional systems can be considered as if "magnets" when their relaxation time becomes extremely long. Glauber predicted that this characteristic time of relaxation should follow an Arrhenius law with an energy barrier $\Delta_{Glauber} \approx 8JS_T{}^2$.[39]

Surprisingly, the first evidence of slow relaxation in a one-dimensional compound has been reported only in 2001 by the group of D. Gatteschi (about 40 years after Glauber's prediction!!). Far from the prototype chain imagined by Glauber, this compound is a ferrimagnetic chain: $Co^{II}(hfac)_2(NITPhOMe)$ (hfac = hexafluoroacetylacetonato, NITPhOMe = 4-methoxyphenyl-4,4,5,5-tetramethylimidazoline-1-oxyl-3-oxide), where $Co(hfac)_2$ and NITPhOMe radical moieties alternately arranged in a helical chain.[40,41] The slow relaxation of the magnetization is induced by the strong anisotropic Co^{II} metal ion and a strong Co^{II}–radical antiferromagnetic interaction. The helical arrangement of the cobalt local anisotropy tensors leads to a complex magnetic behavior superposed on the slow relaxation process. In parallel to this work, an important part of our researches has been devoted to the design of simple chains in order to obtain an experimental model system to study the Glauber's relaxation. In 2002, we reported on a new one-dimensional compound $[Mn_2(saltmen)_2Ni(pao)_2(py)_2](ClO_4)_2$ ($saltmen^{2-}$ = *N*,*N*′-(1,1,2,2-tetramethylethylene)bis(salicylideneiminato), pao^- = pyridine-2-aldoximato, py = pyridine),[42] which can be considered as a chain of ferromagnetically-coupled anisotropic $S_T = 3$ units. As predicted by Glauber, magnetic measurements on this compound revealed the presence of slow relaxation and large field-dependent hysteresis of the magnetization at low temperatures. By analogy to the SMMs, we called this type of materials: Single-Chain Magnet (SCM).[42] This SCM system offers two important advantages: (i) each chain is structurally and magnetically well isolated by the counter anions and bulky ligands, which precludes any magnetic order, and (ii) the local easy axes of the repeating units of chain are all parallel to the unique chain orientation. Therefore, this chain, composed of ferromagnetically-coupled anisotropic $S_T = 3$ units, is the image that we had of the Glauber Ising-type chain and hence supplies us a simple model system to study the magnetic dynamics (i.e., Glauber dynamics). Although the number of SCM materials known[43] is increasing with the discoveries of cyano-bridged Co^{II}–Fe^{III} ferromagnetically-coupled systems,[44] a helical chain of ferromagnetically-coupled Co^{II} system,[45] and a Co^{II}–Cu^{II} antiferromagnetically-coupled system,[46] the previous $Mn^{III}{}_2Ni^{II}$ chain[42] is still to date the simplest system available to probe the Glauber dynamics.

This review is devoted to summarizing our contributions to the growing field of single-chain magnet from the synthetic point of view as well as our contributions on their magnetic properties. Our synthetic strategy to built SCMs has adopted a rational step-by-step approach with pre-designed primary and secondary building blocks (Fig. 2). In order to introduce uni-axial anisotropy, we decided to employ Mn^{III} salen-type units known to possess a strong intrinsic uni-axial anisotropy in their monomers (primary building blocks) and also in their out-of-plane dimeric forms (secondary building blocks).[47] These complexes also act as good coordinating-acceptor building blocks as shown, for example, in many examples of assemblies with polycyanometalate ($[M^{n+}(CN)_m]^{(m-n)-}$).[48,49] Among the salen-type ligands, the *N*,*N*′-(1,1,2,2-tetramethylethylene)bis(salicylideneiminato) (abbreviated saltmen hereafter) reacts with Mn^{III} to form ferromagnetically-coupled out-of-plane dimers with an $S_T = 4$ spin ground state that in some cases exhibit SMM behavior.[14] As a primary coordinating-donor building block, we selected metal (M) oximato complexes that link magnetically to metal ions (M′) or generally to coordinating-acceptors units through an oximate-bridge (M–NO–M′).[50] Using the pyridine-2-aldoximato (pao^-) ligand, we have synthesized new Ni^{II} building blocks: $Ni(pao)_2(L^1)_2$ (L^1 = monodentate N-ligand such as pyridine and its derivatives),[51] $Ni(pao)_2(L^2)$ (L^2 = 2,2′-bipyridine and 1,10-phenanthroline),[52] and $[Ni(Hpao)(bpy)_2](ClO_4)_2$.[53] Thanks to these primary units, secondary building blocks have been obtained: (i) Trinuclear complexes composed of two Mn(saltmen) moieties and one $Ni(pao)_2(L^2)$ unit, i.e. making a [Mn^{III}–ON–Ni^{II}–NO–Mn^{III}] motif, were produced. This type of building blocks acts as a SMM induced by the uni-axial anisotropy and its $S_T = 3$ spin ground state,[20] (ii) Employing $[Mn(saltmen)]^+$ and $[Ni(pao)(bpy)_2]^+$ units produced in-situ a secondary dinuclear [Ni^{II}–NO–Mn^{III}] moiety, which dimerizes to form a tetranuclear [Ni^{II}–NO–Mn^{III}–$(O)_2$–Mn^{III}–ON–Ni^{II}] complex (where –ON– is a oximato bridge and –$(O)_2$– is a bi-phenolate bridge).[53] To form a one-dimensional assembly, secondary trinuclear [Mn^{III}–ON–Ni^{II}–NO–Mn^{III}] building blocks "polymerize" via self-assembly to produce [–$(O)_2$–Mn^{III}–ON–Ni^{II}–NO–Mn^{III}–]$_n$ chains. Along this strategy, we have obtained a family of $Mn^{III}{}_2Ni^{II}$ SCM systems possessing

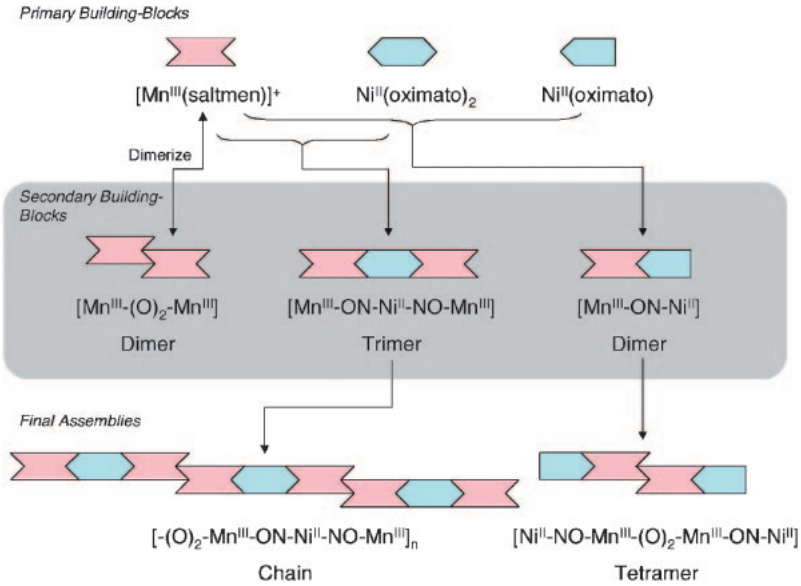

Fig. 2. Schematic representation of step-by-step building-block strategy to construct SCM molecular assemblies, where –NO– is the oximate bridge and $-(O)_2-$ is the bi-phenolate bridge in the out-of-plane dimer form of $[Mn_2(saltmen)_2]^{2+}$. In this diagram, 1:1 alternating chain assemblies shown in Fig. 3a are not described.

an $S_T = 3$ repeating unit: $[Mn_2(saltmen)_2Ni(pao)_2(L^1)_2](A)_2$ ($saltmen^{2-}$ = *N*,*N*′-(1,1,2,2-tetramethylethylene)bis(salicylideneiminato); pao^- = pyridine-2-aldoximato; L^1 = pyridine, 4-picoline, 4-*tert*-butylpyridine, *N*-methylimidazole; and A^- = ClO_4^-, BF_4^-, PF_6^-, and ReO_4^-).[42,54,55]

It is worth noting that this step-by-step synthetic approach to obtain one-dimensional compounds offers the opportunity to modify them easily at the molecular level (metal, ligands, solvents, and counter ions) and therefore to tune finely the magnetic parameters such as intra- or inter-chain magnetic coupling or anisotropy. One is also able to generalize the observed SCM behavior. Moreover, the magnetic characteristics of the primary and secondary building blocks must not be neglected, as they allow a simple estimation of the magnetic parameters that can be directly compared to the ones deduced for the SCM compounds. During the study of the first SCM compound, we suspected that the observed magnetic properties were somehow not completely understood by the Glauber model. Obviously, the obtained one-dimensional materials were not composed (i) of Ising spin units, but a finite anisotropy (zero-field splitting effect, *D*) had to be considered, nor (ii) of infinite chains, but indeed intrinsic crystalline defects were necessary, leading to finite-size chains. Thus, this real SCM system and its physical characteristics were quite far from the idealistic theory. Therefore, our efforts were first dedicated to generalizing the Glauber theory for real systems including finite anisotropy and finite-size chain effects and to studying systematically the magnetic properties of SCM series that validate our theoretical approach.

In this review, we will follow our synthetic road from the primary and secondary building blocks to the final targeted compounds. The Single-Chain Magnet materials will be presented in details together with their remarkable magnetic properties and their interpretations using a generalization of the Glauber model.

1. Synthetic Strategy: Necessary Ingredients to Obtain SCM Behavior

The first question that a chemist asks when he or she is targeting a peculiar physical behavior is "what are the molecular design and physical ingredients necessary to get what I want?" For one to design Single-Chain Magnet materials and before one starts anything, four essential ingredients need to be considered about the elementary spin unit or building block: this needs (i) to be able to connect one-dimensionally, (ii) to be magnetically coupled without complete cancellation of the chain magnetization, and (iii) to possess a strong uni-axial anisotropy (Ising-like). Moreover (iv), the one-dimensional arrangement should be as magnetically isolated as possible, i.e. the magnetic inter-chain interactions must be very weak compared to intra-chain coupling in order to avoid the stabilization of a three-dimensional magnetic order.

So, let's try to give individual answers to these points and to figure out which system could finally meet all of these requirements. First, it appears clear that the elementary units (building blocks) need to have only two available linking sites on both coordinating-acceptor and coordinating-donor moieties to get a one-dimensional arrangement. The remaining coordination sites of the elemental units should hence be controlled by designed blocking ligands. Then, how can we avoid magnetic compensation of the spins along the chain? It is well-known by the chemists working in the field of molecule-based magnetism that antiferromagnetic interaction is, most of the time, active through bridging groups between transition metals. Therefore, a simple approach to avoid the spin-cancellation would be to connect alternately different kinds of spin units (i.e., $S_A \neq S_B$) along the chain as $[\cdots S_A \cdots S_B \cdots S_A \cdots S_B \cdots]$. With this strategy, the coupling mode between spin units (ferro- or antiferromagnetic) does not matter, because the spin cancellation is impossible in both cases. It is noteworthy that the design of a simple regular ferromagnetically-coupled spin chain with

a single kind of spin carrier is still a challenge for the community, because such a chain would be the prototype of the Glauber chain. Indeed Gao and co-workers have reported an example of a homo-spin SCM: $[Co^{II}(2,2'\text{-bithiazoline})(N_3)_2]_n$, in which azide groups bridged anisotropic Co^{II} ions in an end-on geometry to produce ferromagnetic coupling.[45] Nevertheless, the presence of three crystallographically-independent Co sites led to a helical arrangement of spin carriers, which complicated the understanding of its relaxation dynamics.

As with SMMs, the anisotropy is a key ingredient to get slow relaxation of the magnetization in SCM system. Therefore, the choice of the metal ion to be employed and the control of its coordination sphere are very important. Considering the previous ingredients, we have chosen Mn^{III} salen-type complexes as one of two kinds of building units; here, salen^{2-} is the abbreviation of *N*,*N*′-ethylenebis(salicylideneiminato) (Chart 1).[56] Each salen-type Schiff-base molecule acts as a tetradentate ligand, which generally occupies the equatorial plane around an octahedral high spin Mn^{III} ion ($3d^4$, $S = 2$). This type of complex can be viewed in many cases as a *trans*-bi-coordinating-*acceptor* unit with its axial positions available for further coordination (ligand-exchange labile site). The octahedral geometry of these Mn^{III} complexes is usually strongly distorted due to a Jahn–Teller effect. Gerritsen and Sabinsky have experimentally demonstrated that the anisotropy of a Mn^{III} ion depends highly on its Jahn–Teller distortion, leading in most of the cases to a negative zero-field splitting (ZFS) parameter (*D*), in other words, to uni-axial anisotropy.[57] The Jahn–Teller axis corresponds to the easy axis, i.e. the preferential orientation of the magnetic spin on the Mn^{III} complex. When these complexes are assembled into a chain with a *trans*-bridging ligand or *trans*-coordinating-*donor* unit, the individual Mn^{III} Jahn–Teller axes are necessarily aligned to the chain direction (Fig. 3). This topology leads to a simple system with an easy axis of the magnetization parallel to the chain direction.

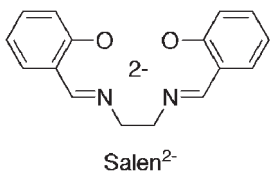

Salen^{2-}

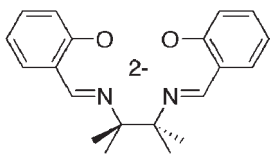

Saltmen^{2-}

Chart 1.

Salen-type ligands are also interesting due to the steric hindrance that is necessary to isolate chains into the materials. As mentioned above (fourth requirement to obtain SCM behavior), the inter-chain interactions must be as weak as possible in order to avoid the stabilization of a three-dimensional magnetic order. The inter-chain interaction is closely associated with the packing arrangement of chains and structural contacts such as π–π stacking or hydrogen bonding in crystal structure. The control of the inter-chain interaction may thus be achieved by design of the right molecular unit, taking into account (i) the metal-surrounding ligands (blocking ligands) for producing a steric hindrance around the chains and (ii) the intercalation of counter ions for occupying evenly the maximum of void space between chains.

Among many derivatives of salen-type ligands known to date, we decided to use saltmen^{2-} tetradentate Schiff-base ligand (Chart 1) and its derivatives (R-saltmen^{2-}) to synthesize new Mn^{III} complexes.[58] The saltmen ligands seem to be slightly bulkier than the salen ligand, but they are still structurally closely related, i.e. the ethylene moiety of the salen being replaced by 1,1,2,2-tetramethylethylene in saltmen. The magnetic properties of these complexes have been reported in details.[58,59] In many cases, the Mn^{III} complexes based on saltmen-type ligand adopt an out-of-plane dimeric form, as shown

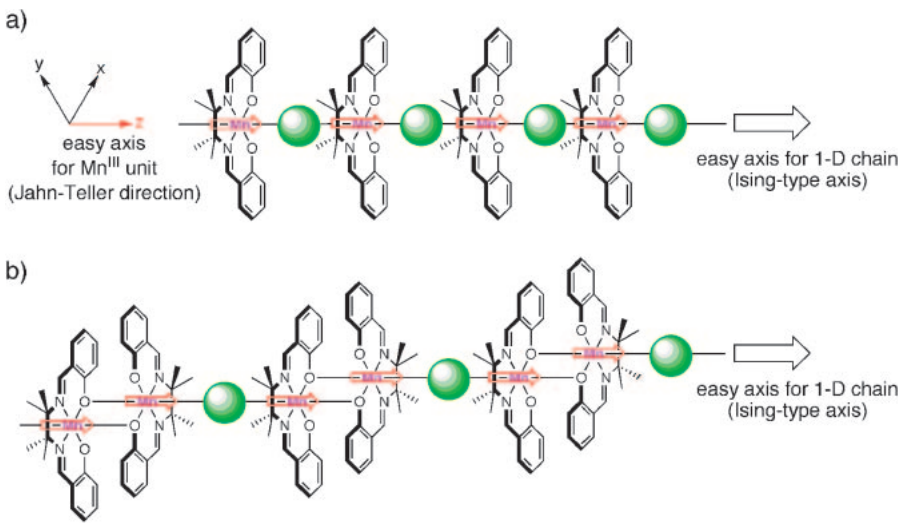

Fig. 3. Schemes of one-dimensional arrangements of Mn^{III} saltmen units (for both monomer and out-of-dimer forms) with linkers (green ball; organic linkers or coordination-donor metal complexes). In both cases, the Jahn–Teller axis of Mn^{III} ions is directed along the one-dimensional assembly inducing the presence of an unique easy-axis for a given chain.

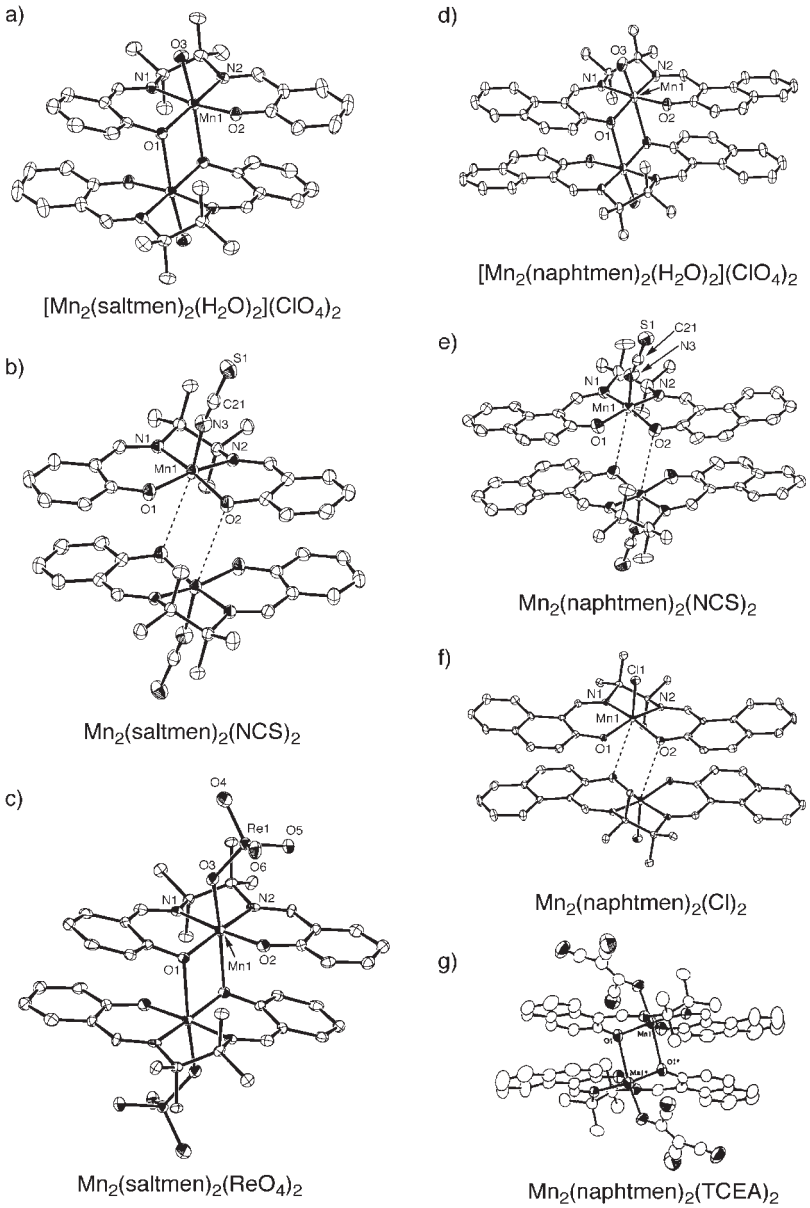

Fig. 4. Structures of out-of-plane dimers of Mn^{III} saltmen- and naphtmen-type compounds (Adapted from Ref. 58. Copyright 2002, RCS; from Ref. 14. Copyright 2004, Wiley-VCH; from Ref. 59. Copyright 1996, Elsevier).

in Fig. 4. These dimers exhibit a strong uni-axial anisotropy and an $S_T = 4$ spin ground state induced by a intra-dimer ferromagnetic coupling. Interestingly, as shown in Fig. 5, the correlation between this ferromagnetic exchange and the Mn···O* distance (O* is the bridging phenolate oxygen) in R-saltmen-based Mn^{III} out-of-plane dimers is almost linear. Table 1 summarizes the pertinent bond distances, angles, and the known magnetic parameters for some R-saltmen- and salen-based dimers.[60–68] Such ferromagnetic exchange can be understood by considering the arrangement of the Mn^{III} ion d-orbitals. The electronic configuration of the high spin Mn^{III} ion in an elongated Jahn–Teller distortion is known to be $(d_{xy})^1$, $(d_{yz})^1$, $(d_{xz})^1$, and $(d_{z^2})^1$ with a $^5B_1$ ground state.[69] The methyl group of saltmen-type ligand acts as an electron donor and enhances the Jahn–Teller orbital splitting. So, the ferromagnetic exchange interaction between Mn^{III} ions is mainly the result of orthogonality between the d_{z^2} and the $d\pi$ orbitals (d_{xy}, d_{yz}, and d_{xz} orbitals). When the Mn···O* distance increases, the ferromagnetic interaction in the out-of-plane dimeric core decreases; the exchange interaction could vanish when the Mn···O* distance reaches ca. 3.8 Å. The correlation between the Mn···Mn distance and the exchange coupling has the same trend.

These characteristics (*trans*-bi-coordination ability, steric hindrance, and anisotropy) illustrate how Mn^{III} saltmen-type complexes could be useful to design SCMs not only in their monomeric form, $[Mn^{III}(saltmen)]^+$ ($S_T = 2$) (Fig. 3a), but also in their dimeric form, $[Mn^{III}{}_2(saltmen)_2]^{2+}$ ($S_T = 4$) (Fig. 3b). Among these dinuclear Mn^{III} building blocks, we have chosen to devote a part of this review to the remarkable magnetic behavior of $Mn_2(saltmen)_2(ReO_4)_2$. This simple dimer behaves as a magnet at the molecular level (SMM) and shows quantum tunneling of the magnetization.[14]

2. $Mn_2(saltmen)_2(ReO_4)_2$: A Di-Nuclear Complex Can Be a SMM

A further proof for the claim that Mn^{III} saltmen dimers are anisotropic building units has been given by our recent report on the SMM behavior in $Mn_2(saltmen)_2(ReO_4)_2$. $[Mn_2(saltmen)_2(H_2O)_2](ClO_4)_2$, and its derivatives, $Mn_2(saltmen)_2(ReO_4)_2$, have an out-of-plane dimeric form (Fig. 4c) with Mn^{III} sites assuming an axial-elongated square bipyramidal six-coordination geometry (the free apical positions are occupied by ReO_4^-) [the average Mn(1)–X bond distance: 1.948(4) Å where X: N or O atom of the $saltmen^{2-}$ ligand, the axial bonds of Mn(1)–O(3) and Mn(1)–O(1*): 2.184(4) and 2.459(4) Å, respectively]. This structural feature is a typical case of Jahn–Teller distortion in Mn^{III} ions surrounded by salen- and R-saltmen-type tetradentate Schiff-base ligands.[58–68] As noted above, the exchange interaction between Mn^{III} ions via a bi-phenolate bridge is ferromagnetic, and a ZFS effect induced by the uni-axial anisotropy (D_{Mn}) of each Mn^{III} ion is observed at low temperatures (Fig. 6). From the estimated values of J and D_{Mn}, the energy diagram could be calculated (inset of Fig. 6) and the energy barrier, Δ/k_B, be-

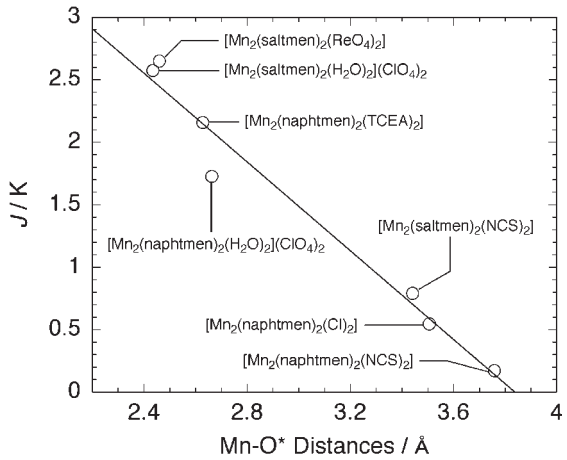

Fig. 5. Correlation between the ferromagnetic exchange parameters J and the Mn–O* distances in Mn^{III} out-of-plane dimers with $saltmen^{2-}$ and $naphtmen^{2-}$ (Adapted from Ref. 58. Copyright 2002, RCS).

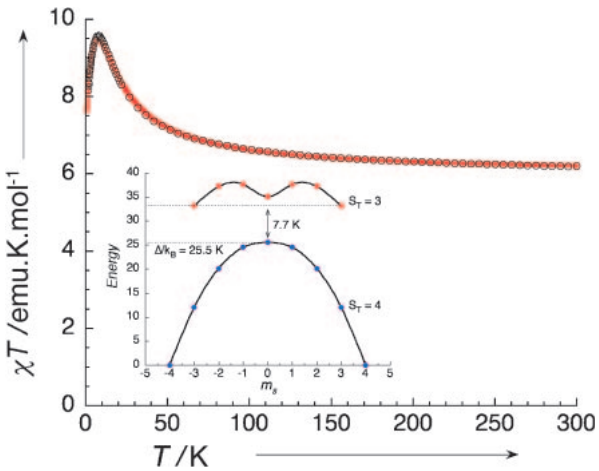

Fig. 6. Temperature dependence of χT product of $Mn_2(saltmen)_2(ReO_4)_2$ under 1 kOe. The red line represents a best simulation using an $S_{Mn} = 2$ dimer model with $g = 2.00$, $J/k_B = +2.65(5)$ K, and $D_{Mn}/k_B = -4.0(2)$ K. Inset: Energy diagram of the two lowest spin states calculated from the fitting of the temperature dependence of the magnetic susceptibility (Reprinted with permission from Ref. 14. Copyright 2004, Wiley-VCH).

Table 1. Pertinent Bond Distances (Å) and Angles (°) for Out-of-Plane Mn^{III} Dimeric Cores and Magnetic Parameters Obtained from the Best Fitting of the Magnetic Susceptibility (F = Ferromagnetic Interaction, AF = Antiferromagnetic Interaction)

	Structural aspects						Magnetic parameters				
Compd[a)]	Mn–O	Mn–O*	O–Mn–O*	Mn–O–Mn*	Mn···Mn*		g	J/k_B [K]	D_{Mn}/k_B [K]	zJ/k_B [K]	Ref.
I	1.909(2)	2.434(2)	78.42(10)	101.58(10)	3.381(1)	*F*	1.93	2.58	−3.64	−1.14	58
II	1.872(2)	3.441(2)	83.76(8)	96.24(8)	4.0923(8)	*F*	1.99	0.79	−1.80		58
III	1.913(4)	2.459(4)	81.5(1)	98.5(2)	3.330(1)	*F*	2.00	2.65	−4.00		14
IV	1.896(3)	2.662(3)	79.4(1)	100.6(1)	3.541(1)	*F*	1.96	1.73	−0.55		58
V	1.877(2)	3.758(3)	83.43(10)	96.57(10)	4.3885(9)	*F*	2.03	0.17	−1.44		58
VI	1.892(5)	3.505(5)	85.8(2)	94.2(2)	4.102(2)	*F*	2.04	0.55	−2.69		58
VII	1.90(1)	2.85(1)	79.9(5)	100.1(5)	3.693(6)	*F*					48b
VIII	1.904(3)	2.627(3)	81.1(1)	98.9(1)	3.475(2)	*F*	2.01	2.16		−0.50	59
IX	1.878(9)	3.103(5)	88.9(2)	91.1(2)	3.658(2)	*F*					67
X	1.901(5)	2.412(6)	79.42(21)	100.58(22)	3.334(3)	*F*	2	9.06	−2.45		68
XI	1.912(3)	2.305(2)	76.6(1)	103.4(1)	3.318(1)	*AF*		−2.42			62
XII	1.906(6)	2.419(7)	—	—	3.350(3)	*AF*					64
XIII	1.891(3)	2.490(3)	80.7(1)	99.3(1)	3.361(2)	*AF*					65
XIV	1.880(6)	2.750(6)	81.3(2)	98.7(2)	3.558(3)	*AF*					66a, 47

a) **I**: $[Mn_2(saltmen)_2(H_2O)_2](ClO_4)_2$, **II**: $[Mn_2(saltmen)_2(NCS)_2]$, **III**: $[Mn_2(saltmen)_2(ReO_4)_2]$, **IV**: $[Mn_2(naphtmen)_2(H_2O)_2](ClO_4)_2$, **V**: $[Mn_2(naphtmen)_2(NCS)_2]$, **VI**: $[Mn_2(naphtmen)_2(Cl)_2]$, **VII**: $[Mn(saltmen)]_4[Fe(CN)_6]ClO_4$, **VIII**: [Mn(naphtmen)(TCEA)] (TCEA = tricyanoethenolate), **IX**: [Mn(salen)Cu(A)]BPh_4 (H_2A = 4-(6-methyl-8-oxo-2,5-diazanonane-1,5,7-trienyl)imidazole), **X**: $[Mn(salen)(H_2O)]_2(ClO_4)_2$, **XI**: $[Mn(L)(H_2O)]_2(ClO_4)_2$ (L = *N*-(acetylacetonylidene)-*N*′-(α-methylsalicylidene)ethylenediamine), **XII**: $[Mn_2(bsalen)_2(H_2O)_2](ClO_4)_2$ (bsalen = *N*,*N*′-ethylenebis(5-bromosalicylideneiminato) dianion, **XIII**: $[Mn(salen)(H_2O)]_2(ClO_4)_2 \cdot H_2O$, **XIV**: [Mn(salen)(NCS)].

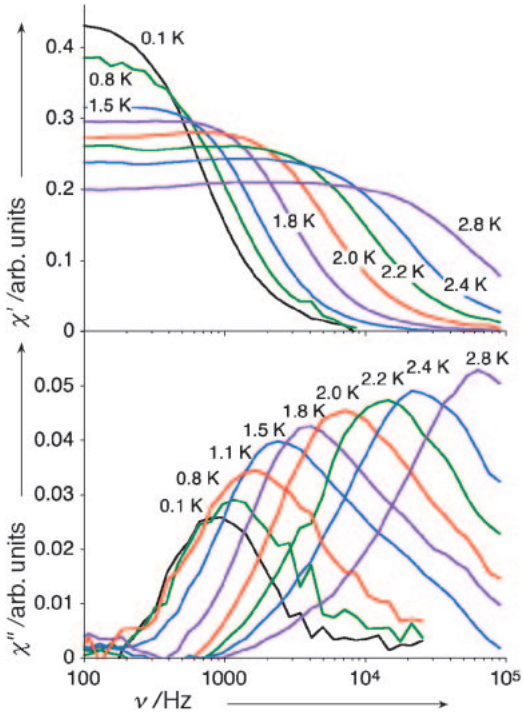

Fig. 7. Frequency dependence of the in-phase (χ') and out-of-phase (χ'') ac susceptibility of $Mn_2(saltmen)_2(ReO_4)_2$ at temperature below 2.8 K at zero dc field and with an amplitude of the ac field of 5 Oe. These measurements have been done on a single crystal aligned with one of the two easy directions (Reprinted with permission from Ref. 14. Copyright 2004, Wiley-VCH).

tween $m_s = \pm 4$ levels was estimated to be 25.5 K. As $\Delta = |D_{Mn2}|S_T^2$ for SMMs with an integer S_T spin, D_{Mn2} was estimated at -1.59 K, where D_{Mn2} is the uni-axial anisotropy for the Mn^{III} dimer. In agreement with this estimation, the best-fitting of the reduced magnetization M vs H/T plot leads to $D_{Mn2}/k_B = -1.63$ K and consequently to a theoretical energy barrier, Δ, of 26 K.

Alternating-current (ac) susceptibility measurements are an important tool to probe magnetic relaxations and thus to characterize SMM behavior. As expected for SMMs, ac measurements on $Mn_2(saltmen)_2(ReO_4)_2$ at different temperatures show a strong frequency dependence for both components of the ac susceptibility (the real part χ' and the imaginary part χ'', Fig. 7). A single relaxation process has been identified and its relaxation time (τ) has been deduced from the maximum of the χ'' versus ν curves ($\tau = 1/(2\pi\nu_{max})$), plotted as a function of $1/T$ (Fig. 8). Between 4 and 1.9 K, the relaxation follows an Arrhenius law (see inset of Fig. 8) with $\Delta_{eff}/k_B = 16$ K and $\tau_0 = 8 \times 10^{-9}$ s. On the other hand, below 1.9 K, τ saturates, becoming truly temperature independent at 1.9×10^{-4} s below 0.6 K. This feature is characteristic of SMM behavior when quantum tunneling of the magnetization (QTM) is dominant between the lowest m_{sT} levels of the ground state. As a result of the QTM, the experimental energy barrier, Δ_{eff}, is lower than the expected value calculated from D_{Mn2} ($\Delta/k_B = 26$ K). Associated with the slow relaxation, hysteresis loops of the magnetization have been observed between 0.04 and 2 K when applying the external field along

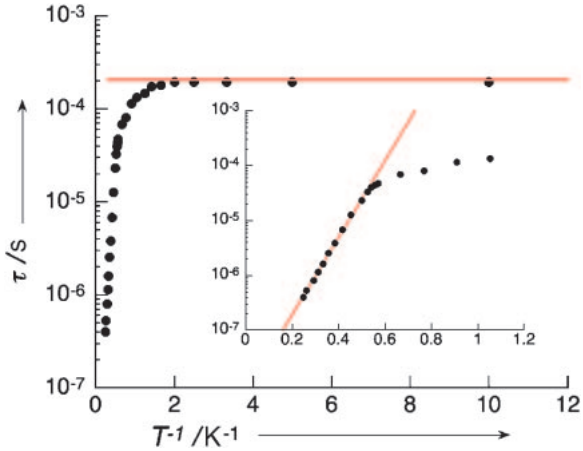

Fig. 8. Relaxation time (τ) versus $1/T$ plot for $Mn_2(saltmen)_2(ReO_4)_2$. Inset: View of the high temperature region of the τ versus $1/T$ plot to emphasize the Arrhenius behavior (Reprinted with permission from Ref. 14. Copyright 2004, Wiley-VCH).

the easy axis of molecule directions (Jahn–Teller direction).

These data indicated that a simple out-of-plane Mn^{III} dimer, $Mn_2(saltmen)_2(ReO_4)_2$, is an SMM and indirectly that mono- or dinuclear Mn^{III}/saltmen complexes could be useful uni-axial anisotropic building units to design SCM systems. Furthermore, these conclusions let us imagine a new synthetic strategy to design SCMs by coupling ferromagnetically SMMs in one-dimension.

3. Ni^{II} Oximato Complexes: Our Linking Building Unit

In our synthetic strategy, the design of one-dimensional structures is achieved by connecting two different kinds of building units, i.e., coordinating-*acceptor* building units and coordinating-*donor* building units. As introduced in the previous section, we have established that Mn^{III} salen- or saltmen-type complexes are good candidates to be coordinating-*acceptor* units (with a *trans*-bi-coordination ability, a good steric hindrance, and a large uni-axial anisotropy). So, the next step was to choose a coordinating-donor unit. Among the numerous possible complexes, we have selected a family of Ni^{II} oximato complexes (Fig. 9): $Ni^{II}(pao)_2(L^1)_2$ (L^1 = pyridine,[70] 4-picoline, 4-ethylpyridine, 4-*tert*-butylpyridine, *N*-methylimidazole), $Ni^{II}(pao)_2(L^2)$ (L^2 = 2,2′-bipyridine, 1,10-phenanthroline), and $[Ni^{II}(pao)(bpy)_2]^+$. The Ni^{II} complexes, $Ni^{II}(pao)_2(L^1)_2$ and $Ni^{II}(pao)_2(L^2)$ shown in Figs. 9a and 9b, respectively, consist of two pyridine-2-aldoximato (pao^-) and two monodentate N-ligands such as pyridine derivatives for *trans*-type species (Fig. 9a) or one bidentate N-ligand such as 2,2′-bipyridine or 1,10-phenanthroline for NO-*trans*-type species (Fig. 9b). The coordination sphere around the Ni^{II} ion is slightly distorted octahedral which induces an $S = 1$ ground spin state ($^3A_{2g}$ term). These complexes are neutral, and the oxygen atom of the oximato groups is able to coordinate to metal ions and therefore to bridge the Ni^{II} centre to a given metal (M) ion, forming Ni^{II}–NO–M links.[50g] Depending on the metals, the oximate bridge mediates significant magnetic exchanges.[50] Nevertheless, no examples of structurally-characterized polymeric compounds with the oximate-bridge

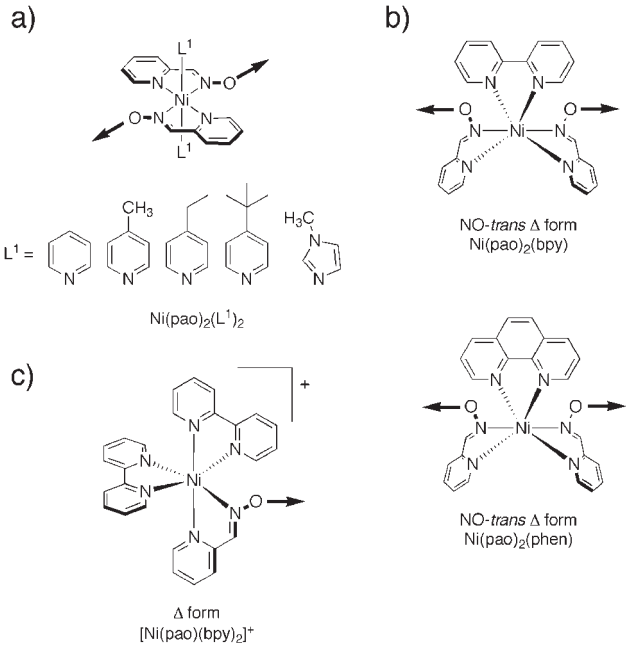

Fig. 9. Ni^{II}/pao complexes acting as coordinating-donor building units (or linking units). a) *trans*-Type building unit, $Ni(pao)_2(L^1)_2$, where L^1 is pyridine (py), 4-picoline (pic), 4-ethylpyridine (Etpy), 4-*tert*-butylpyridine (*t*-Bupy), and *N*-methylimidazole (Meim). b) NO-*trans*-type building unit, $Ni(pao)_2(bpy)$ and $Ni(pao)_2(phen)$, where bpy and phen are 2,2′-bipyridine and 1,10-phenanthroline, respectively. c) Terminal building unit, $[Ni(pao)(bpy)_2]^+$. Figures b) and c) only represent Δ form while the racemic species were synthesized in our work.

have been reported until our 1-D systems ($[Mn_2(saltmen)_2Ni(pao)_2(L^1)_2](A)_2$) have been revealed.[42,71] The complexes depicted in Figs. 9a and 9b have two NO groups in *trans*-configuration and could be thus used as a linear-type coordinating-donor building-block between two metallic units as M–ON–Ni^{II}–NO–M. As we will show later in this review, Mn^{III}–Ni^{II}–Mn^{III} trimers (Section **5**) and Mn^{III}/Ni^{II} chains (Section **6**) have been successfully synthesized using $Ni^{II}(pao)_2(L^2)$ and $Ni^{II}(pao)_2(L^1)_2$, respectively, in association with the Mn^{III}/saltmen unit (Figs. 10a and 10b, respectively). It is also interesting to note that the neutrality of the Ni units allows the final product to keep the counter anions introduced from the Mn^{III} precursor. In the case where the SCM materials are targeted, the presence of these counter anions that are intercalated into the void space between the chains, would help indubitably to minimize the inter-chain interactions. As mentioned in Section **1**, this point is crucial (fourth condition) to obtain SCM materials and to prevent the stabilization of the magnetic order.

On the other hand, $[Ni^{II}(pao)(bpy)_2]^+$ shown in Fig. 9c is composed of only one pao^- ligand and two bpy ligands, forming an octahedral cationic building-block.[53] While $Ni(pao)_2(L^1)_2$ and $Ni(pao)_2(L^2)$ are linking units, this complex acts as a terminal moiety allowing the synthesis of heterometallic oligomeric complexes. Actually, assembly reactions with Mn^{III}/(5-R-saltmen) building-blocks gave a series of tetranuclear complexes: $[Mn(5\text{-R-saltmen})Ni(pao)(bpy)_2]_2(ClO_4)_4$ (R = H, Cl, Br, MeO) (Figs. 2 and 10c). This family of compounds and also the previous mentioned trinuclear complexes are, from the magnetic point of view, relatively simple and thus allowed us to get easily quantitative estimations of the magnetic exchanges through Mn^{III}–ON–Ni^{II} and Mn^{III}–$(O)_2$–Mn^{III} bridges. The next two sections will be devoted to the oligomeric species which can be viewed as elementary compo-

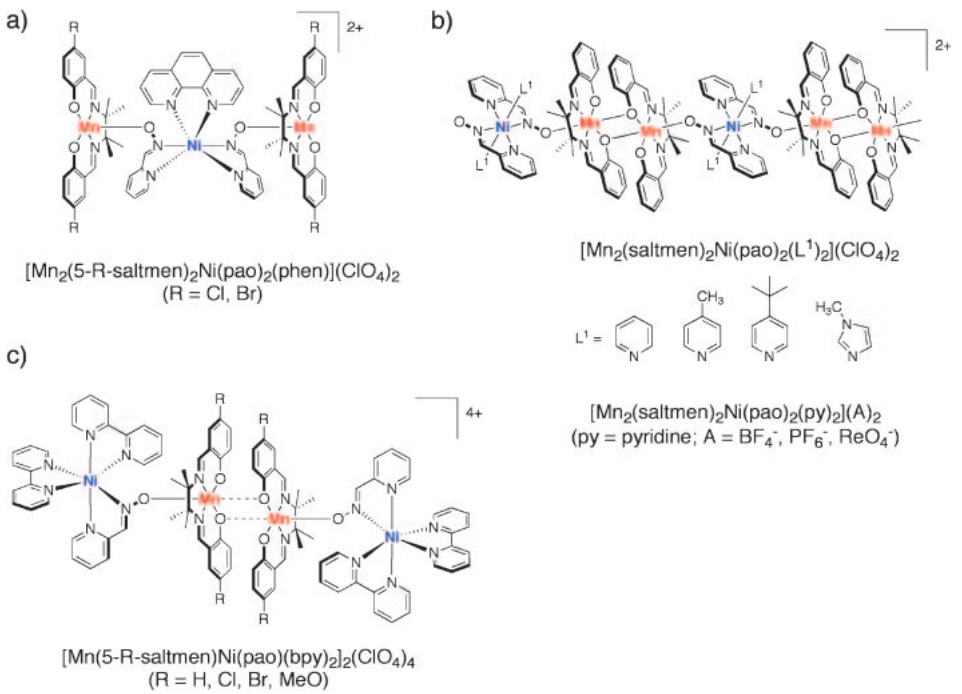

Fig. 10. Different possible assemblies of Mn^{III}/saltmen-type complexes and Ni^{II}/pao complexes.

nents of the $[-Mn^{III}-ON-Ni^{II}-NO-Mn^{III}-(O)_2-]_n$ chains (Fig. 10b) described in Section **6**.

4. Tetranuclear Ni^{II}–Mn^{III}–Mn^{III}–Ni^{II} Complexes

The assembly reaction of $[Ni(pao)(bpy)_2]^+$ with $[Mn_2(5\text{-R-saltmen})_2(H_2O)_2](ClO_4)_2$ in a molar ratio of 2:1 produced isostructural linear tetramers independently on the 5-R substituent (R = H, Cl, Br, MeO): $[Mn(5\text{-R-saltmen})Ni(pao)(bpy)_2]_2(ClO_4)_4$.[53] As shown in Fig. 11, the linear-type tetranuclear complexes have an inversion center in the midpoint of $[Mn_2(5\text{-R-saltmen})_2]^{2+}$ dimeric core. This centro-symmetry is induced by the presence of the Δ and Λ isomer forms of the $[Ni(pao)(bpy)_2]^+$ moieties. Mn^{III} ions display a strongly distorted octahedral geometry with a Jahn–Teller axis along the bridging direction. This result suggests that the $[Ni^{II}$–NO–$Mn^{III}]$ dinuclear unit is present in solution and can be thus considered as a secondary building block, as shown in Fig. 2.

The dc magnetic susceptibility measurements on polycrystalline samples of these compounds produced the same magnetic behavior along the series i.e., strong antiferromagnetic interaction between Mn^{III} and Ni^{II} ions via an oximate bridge and weak ferromagnetic interaction between two Mn^{III} ions via a bi-phenolate bridge. The χT vs T plot was simulated by the isotropic Heisenberg spin Hamiltonian for the tetramer unit, $H = -2J_{Mn-Ni}(S_{Mn(1)} \cdot S_{Ni(1)} + S_{Mn(1^*)} \cdot S_{Ni(1^*)}) - 2J_{Mn-Mn}(S_{Mn(1)} \cdot S_{Mn(1^*)})$, taking into account inter-tetramer magnetic interactions (zJ) treated in the frame of the mean-field approximation.[72] The best-sets of parameters obtained are summarized in Table 2. This study gave the magnitude of the magnetic interactions $J_{Mn-Ni}/k_B \sim -26$ K via the –NO– bridge and $J_{Mn-Mn}/k_B < +1$ K via the bi-phenolate bridge, yielding an $S_T = 2$ spin ground state (note that these tetramers do not exhibit SMM behavior above 1.8 K). Both exchange couplings were consistently found in the SCM compounds built on ferromagnetically-coupled $[Mn^{III}$–ON–Ni^{II}–NO–$Mn^{III}]$ tri-nuclear units (see Section **6**). In the next section, we will confirm the magnitude J_{Mn-Ni} in a series of isolated $[Mn^{III}$–ON–Ni^{II}–NO–$Mn^{III}]$ trinuclear complexes that are also described as secondary building blocks and in-situ precursors of SCMs (Fig. 2).

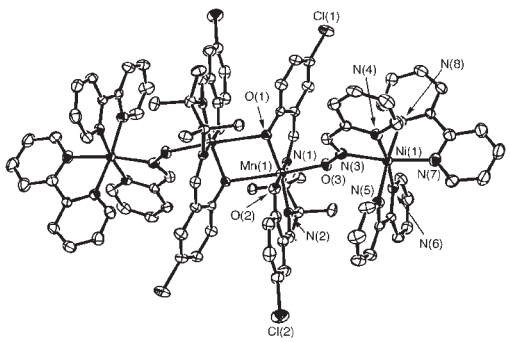

Fig. 11. ORTEP view of a tetramer $[Mn(5\text{-Cl-saltmen})Ni(pao)(bpy)_2]_2(ClO_4)_4$ (Reprinted with permission from Ref. 53. Copyright 2004 The American Chemical Society).

Table 2. Magnetic Parameters for the Tetramers $[Mn(5\text{-R-saltmen})Ni(pao)(bpy)_2]_2(ClO_4)_4$ (R = H, Cl, Br, MeO) Obtained from Simulation of χT Using a Ni–Mn–Mn–Ni Tetramer Model with Inter-molecular Interactions[53]

Compd	g_{av}	J_{Ni-Mn}/k_B [K]	J_{Mn-Mn}/k_B [K]	zJ/k_B [K]
H	2.04(1)	−23.7(2)	+0.90(5)	−0.23(2)
Cl	2.04(1)	−26.1(2)	+0.70(5)	−0.20(2)
Br	2.04(1)	−25.1(2)	+0.80(5)	−0.23(2)
MeO	1.96(1)	−24.4(2)	+0.40(5)	−0.18(2)

5. Mn^{III}–Ni^{II}–Mn^{III} Trinuclear SMM Complexes

As mentioned before in Section **2**, one of our strategies to design SCM is based on the idea to arrange SMMs ferromagnetically in one dimension. Indeed, SMMs possess all of the desired intrinsic characteristics (uni-axial anisotropy, high-spin ground state) needed for a SCM building block (unit). When we discovered the SMM properties of $[Mn^{III}$–ON–Ni^{II}–NO–$Mn^{III}]$ trinuclear complexes, we realized that this approach was already successful and will promote development to design future SCM systems rationally.

If we look more closely at the SCM systems, $[Mn_2(saltmen)_2Ni(pao)_2(L^1)_2](A)_2$, described in Section **6**, we realize that they are obtained from the controlled reaction between an out-of-plane Mn^{III} dinuclear unit and a Ni^{II} oximato moiety as:

$$\cdots\text{–}[ON\text{–}Ni^{II}\text{–}NO]\text{–}[Mn^{III}\text{–}(O)_2\text{–}Mn^{III}]$$
$$\text{–}[ON\text{–}Ni^{II}\text{–}NO]\text{–}[Mn^{III}\text{–}(O)_2\text{–}Mn^{III}]\text{–}\cdots. \quad (A)$$

The chain can be thus viewed as an alternating chain of Mn_2 and Ni moieties. Nevertheless, this view is not relevant to describing the magnetic properties of these one-dimensional compounds. In order to get the magnetic topology of the system, the magnitude of the exchange interactions needs to be considered. As introduced in the previous sections, the exchange interaction between two Mn^{III} ions via the bi-phenolate bridge is relatively weak and ferromagnetic with $J/k_B < +3$ K[14,53,58,59] (in the tetramers, it was evaluated to be $J/k_B < +1$ K).[53] On the other hand, the exchange interaction between Ni^{II} and Mn^{III} ions via the oximate bridge is antiferromagnetic and is estimated to be approximately ~ -26 K,[53] which is much stronger than the exchange interaction between Mn^{III} ions. Therefore, if one includes the magnetic interactions, the magnetic topology of the system can be clearly illustrated by the following scheme:

$$\cdots\text{–}[Mn^{III}\text{–}ON\text{–}Ni^{II}\text{–}NO\text{–}Mn^{III}]\text{–}(O)_2$$
$$\text{–}[Mn^{III}\text{–}ON\text{–}Ni^{II}\text{–}NO\text{–}Mn^{III}]\text{–}(O)_2\text{–}\cdots. \quad (B)$$

The repeating unit of chain that will be helpful to discuss the magnetic properties is hence the $[Mn^{III}$–ON–Ni^{II}–NO–$Mn^{III}]$ trinuclear moiety (Fig. 12). Interestingly, this trinuclear unit is found isolated in a series of materials: $[Mn_2(5\text{-R-saltmen})_2Ni(pao)_2(phen)](ClO_4)_2$ (R = Cl, Br) (Fig. 10a). These discrete complexes yield an $S_T = 3$ spin ground state and exhibit SMM behavior (vide infra).[20] Thus, this result illustrates nicely that the use of SMM as building blocks is an efficient and convenient approach for the rational synthesis of SCMs.

The linear-type trinuclear compounds $[Mn_2(5\text{-R-saltmen})_2Ni(pao)_2(phen)](ClO_4)_2$ (R = Cl, Br) have been synthesized by the assembly reactions of $[Mn_2(5\text{-R-saltmen})_2(H_2O)_2](ClO_4)_2$ (R = Cl, Br) with $Ni(pao)_2(phen)$ in a molar ratio of

1:2 in a MeOH/H_2O solution. The use of the $Ni(pao)_2(bpy)$ building-block instead of $Ni(pao)_2(phen)$ leads, depending on the reaction conditions, to one-dimensional compounds or mixtures of 1-D materials and trinuclear complexes (Fig. 13). This result highlights how the type of ligand (5-R-saltmen or bpy/phen) and its properties (the ligand-field effect on a metal center and the weak ligand-, counter anion-, solvent-, and ligand-interactions) influences dramatically the final architecture in these systems.

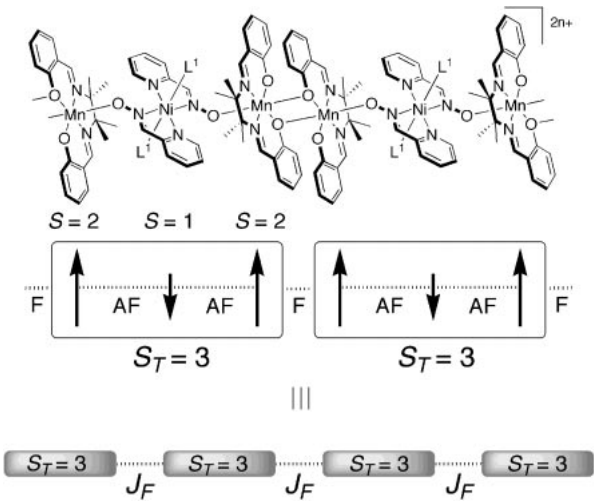

Fig. 12. Schematic representation of the magnetic system: $[Mn_2(saltmen)_2Ni(pao)_2(L^1)_2](A)_2$ (L^1 = monodentate ligand, A^- = counter anion). The $[Mn^{III}–Ni^{II}–Mn^{III}]$ unit exhibits an $S_T = 3$ spin ground state. These units connect ferromagnetically via a bi-phenolate bridge along the chain.

Compounds $[Mn_2(5\text{-R-saltmen})_2Ni(pao)_2(phen)](ClO_4)_2 \cdot n(solvent)$ (R = Cl, Br) are isostructural (Fig. 14). The asymmetrical cationic trimer consists of two $[Mn^{III}(5\text{-R-saltmen})]^+$ groups (R = Cl, Br) and a $Ni^{II}(pao)_2(phen)$ unit linked via oximate bridges of the Ni^{II} moiety, thus forming a $[Mn^{III}–ON–Ni^{II}–NO–Mn^{III}]$ linear motif. The oximato functions of $Ni(pao)_2(phen)$ moiety coordinate to Mn^{III} ion of $[Mn(5\text{-R-saltmen})]^+$ groups on their apical position. Whereas many of Mn^{III} sites in salen- and saltmen-type compounds have a square-bipyramidal coordination geometry with a Jahn–Teller distortion, Mn ions in these trinuclear compounds assume a square-pyramidal geometry (the equatorial Mn–X bond distances (X = N or O of the 5-R-saltmen^{2-} ligand): 1.859–1.990 Å; the apical Mn–O bond distances: 2.059–2.065 Å). Such square-pyramidal geometry is also a case of Jahn–Teller distortion. The vacant apical position is weakly in contact with the 5-R (R = Cl, Br) groups of neighboring trinuclear units with Mn···X (X = Cl, Br) distances of 3.347–3.561 Å; however, these compounds function magnetically as discrete units.

As shown in Fig. 15, the χT product gradually decreases from 300 K to a minimum at ca. 72 K. Below 72 K, χT reaches a maximum at 22 K and then decreases until 1.82 K. Based on the trinuclear nature of the compounds, this behavior was simulated using a $Mn^{III}–Ni^{II}–Mn^{III}$ trimer model ($S_{Mn} = 2$, $S_{Ni} = 1$) with the following Heisenberg Hamiltonian:

$$H = -2J\{S_{Mn1} \cdot S_{Ni} + S_{Ni} \cdot S_{Mn2}\} + g\mu_B S_{Tz} H_z, \qquad (1)$$

where J is the exchange interaction between Mn^{III} and Ni^{II} ions via the –ON– bridge, S_T refers to the total spin operator

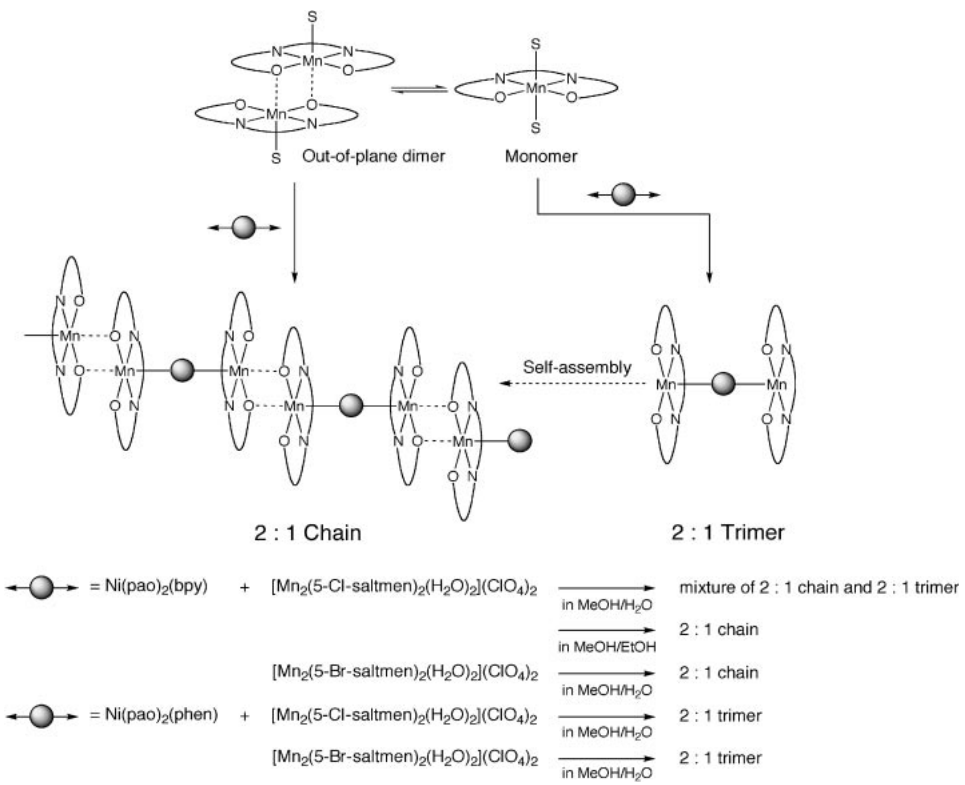

Fig. 13. Reaction scheme of the assemblies of $[Mn_2(5\text{-R-saltmen})_2(H_2O)_2](ClO_4)_2$ with $Ni(pao)_2(bpy)$ and $Ni(pao)_2(phen)$.

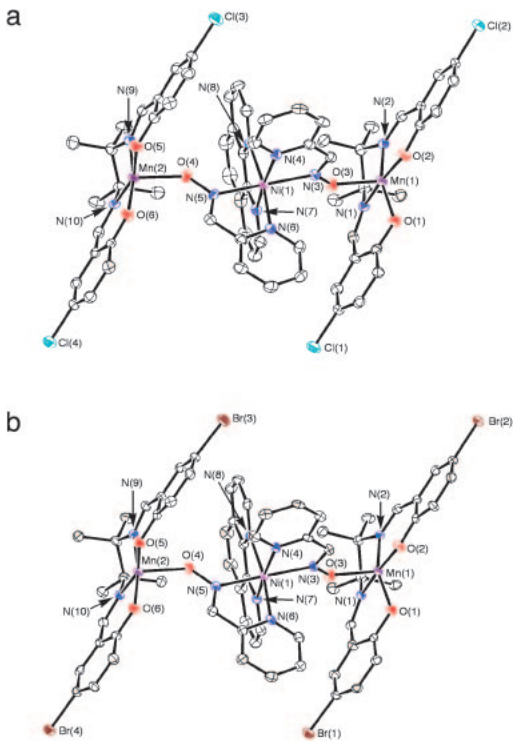

Fig. 14. Structure of cation [Mn–Ni–Mn] trinuclear unit in $[Mn_2(5\text{-R-saltmen})_2Ni(pao)_2(phen)](ClO_4)_2 \cdot n(solvent)$ (R = Cl, **Compd 1**: part a; Br, **Compd 2**: part b) with atomic numbering scheme for selected atoms (50% probability thermal level). Hydrogen atoms are omitted for clarity (Reprinted with permission from Ref. 20. Copyright 2005, Wiley-VCH).

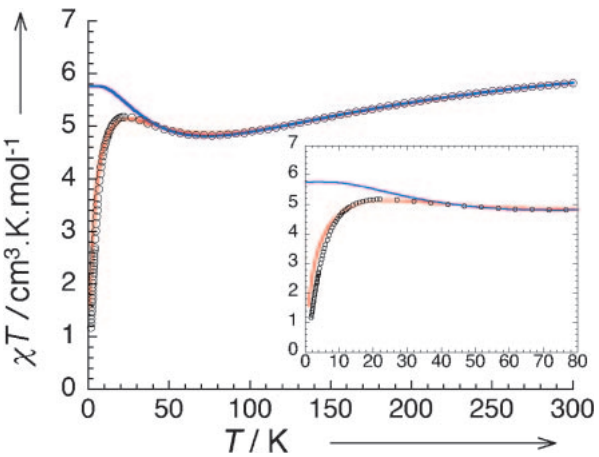

Fig. 15. Temperature dependence of χT product for $[Mn_2(5\text{-Cl-saltmen})_2Ni(pao)_2(phen)](ClO_4)_2$ at 1000 Oe. The solid blue and red lines are the fits using Heisenberg Mn–Ni–Mn trimer model and this same model taking account inter-trimer interactions in mean field approximation, respectively. Inset: Enlarged view of the low temperature region (Reprinted with permission from Ref. 20. Copyright 2005, Wiley-VCH).

of the trimer as $S_T = S_{Mn1} + S_{Ni} + S_{Mn2}$ and S_{Tz} is the projection of S_T along the magnetic field applied in the z direction, H_z. This model simulates well the temperature dependence of χT product from 300 to 45 K and leads to $J/k_B \sim -22$ K (blue line in Fig. 15). Below 45 K, inter-trimer interaction and/or ZFS effects become relevant and should be considered. Therefore, as a first approach, inter-trimer interactions have been introduced, taking into account the mean field approximation:[72]

$$\chi = \frac{\chi_{trimer}}{1 - \frac{2zJ'}{Ng^2\mu_B^2}\chi_{trimer}}, \quad (2)$$

where z is the number of next neighbour trimers and J' is the average inter-trimer magnetic interaction between trinuclear complexes. As shown by the red line in Fig. 15, this model reproduced qualitatively well the magnetic data. The magnetic parameters are summarized in Table 3. It is worth noticing that this antiferromagnetic interaction (J) between Mn^{III} and Ni^{II} ions via the –ON– bridge leads to an $S_T = 3$ spin ground state for both trinuclear compounds. As seen in Fig. 15 below 10 K, antiferromagnetic interactions between trimers evaluated around −0.2 K are not able to completely reproduce the experimental data, indicating that the anisotropy may be relevant to improve the model. Therefore, the anisotropy for the trimer, D, was evaluated from the field dependence of the magnetization at $D/k_B \sim -2.4$ K for both trinuclear compounds (Table 3).[20]

Table 3. Magnetic Characteristics of the Trinuclear Compounds $[Mn_2(5\text{-R-saltmen})_2Ni(pao)_2(phen)](ClO_4)_2$ (R = Cl, Br)[20]

	Cl	Br
J/k_B [K]	−24.3(1)	−24.0(1)
g	2.00(2)	1.97(2)
D/k_B [K][a]	−2.4(5)	−2.4(5)
D/k_B [K][b]	−2.30(5)	−2.31(5)
zJ'/k_B [K][c]	−0.18(2)	−0.19(2)
zJ'/k_B [K][a]	−0.22(2)	−0.21(2)
Δ/k_B [K][d]	21.1(1)	21.2(1)
τ_0 [s][e]	$1.2(1) \times 10^{-7}$	$1.5(1) \times 10^{-7}$
Δ_{eff}/k_B [K][e]	18.3(1)	18.2(1)

a) From the analysis of M vs H curves. b) From the reduced magnetization plots. c) From the analysis of the temperature dependence of the magnetic susceptibilities. d) Calculated from the average value of the D parameters reported in this table. e) Deduced from the analysis of the relaxation time deduced with ac susceptibility measurements.

As observed for SMMs, the presence of uni-axial anisotropy, D, creates an energy barrier, $\Delta/k_B = |D|S_T^2$, between the two $m_s = \pm 3$ levels of the $S_T = 3$ ground state. From the previous magnetic characteristics, Δ/k_B can be estimated to be around 21 K (Table 3). Based on this result, we investigated the possibility of slow magnetization relaxation, i.e. SMM behavior, in these compounds by ac susceptibility measurements. In-phase (χ') and out-of-phase (χ'') components of the ac susceptibility are shown in Fig. 16 for $[Mn_2(5\text{-Cl-saltmen})_2Ni(pao)_2(phen)](ClO_4)_2$ (note that similar results have been obtained with R = Br). As expected for a SMM, both χ' and χ'' components are strongly frequency (ν) dependent and a single relaxation mode of the magnetization is observed. Its characteristic time follows an activated behavior (Arrhenius

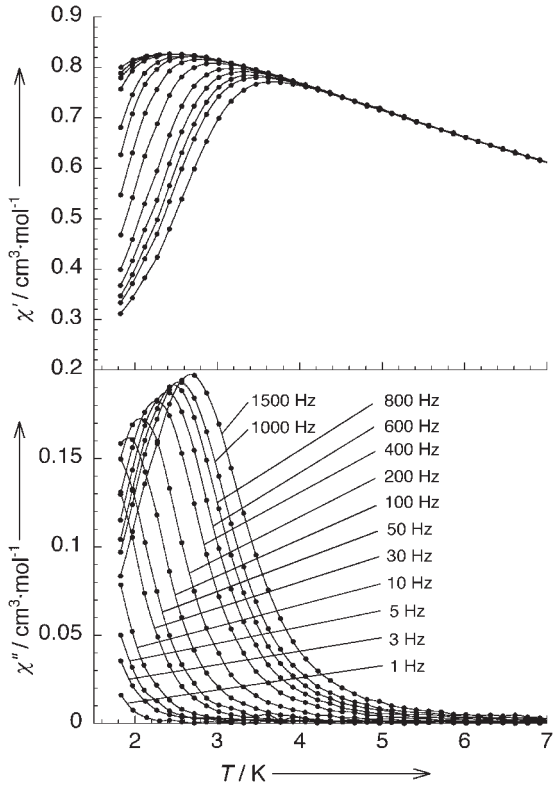

Fig. 16. Temperature and frequency dependence of the real (χ') and imaginary (χ'') parts of the ac susceptibility for $[Mn_2(5\text{-Cl-saltmen})_2Ni(pao)_2(phen)](ClO_4)_2$. The solid lines are guide for the eyes (Reprinted with permission from Ref. 20. Copyright 2005, Wiley-VCH).

law) between 3 and 1.8 K with Δ_{eff} value of 18.3(1) and 18.2(1) K and pre-exponential factors, τ_0, of $1.2(1) \times 10^{-7}$ and $1.5(1) \times 10^{-7}$ s for the trinuclear compounds with R = Cl and R = Br, respectively. The fact that the experimental energy gaps (Δ_{eff}) are lower than the values $\Delta/k_B = 21$ K calculated from D and S_T has been attributed to the quantum tunneling of the magnetization (QTM). Indeed as explained in the case of $Mn_2(saltmen)_2(ReO_4)_2$ (Section **2**), this alternative pathway of relaxation "short-cuts" the thermal energy barrier and an effective Δ_{eff} value is obtained that is lower than the one deduced from $\Delta = |D|S_T^2$ (this regime is also called thermally-assisted QTM).[13a,14]

In summary, we have shown in this section that $[Mn_2(5\text{-R-saltmen})_2Ni(pao)_2(phen)](ClO_4)_2 \cdot n(solvent)$ (R = Cl, Br) possess a $[Mn^{III}\text{–ON–}Ni^{II}\text{–NO–}Mn^{III}]$ trinuclear core, a strong uni-axial anisotropy, and an $S_T = 3$ spin ground state. Furthermore, these characteristics induce SMM behavior with a thermally assisted QTM regime. As these trinuclear units can be viewed as the repeating unit (secondary building block in Fig. 2) of the $[Mn_2(saltmen)_2Ni(pao)_2(L^1)_2](A)_2$ SCM compounds (Section **6**), this result demonstrates that SCMs can be designed by connecting ferromagnetically SMMs in one dimension. This strategy is currently our main research project as we hope in a near future to obtain with this approach new SCMs with high blocking temperatures.

6. A Family of Ferromagnetic Single-Chain Magnets

In 2002, we have reported the slow relaxation of the magnetization in a one-dimensional material: $[Mn_2(saltmen)_2Ni(pao)_2(py)_2](ClO_4)_2$.[42] Starting from this compound, we have developed two types of synthetic strategy to obtain a series of materials with a modulation of the magnetic chain neighborhood: (i) We have substituted L^1 ligands on the Ni^{II} metal ion by several N-type ligands: $Ni(pao)_2(L^1)_2$ (L^1 = pyridine, 4-picoline, 4-*tert*-butylpyridine, *N*-methylimidazole) and reacted this coordinating-donor building block with the coordinating-acceptor complex: $[Mn_2(saltmen)_2(H_2O)_2](ClO_4)_2$. Following this approach, the family of compounds: $[Mn_2(saltmen)_2Ni(pao)_2(L^1)_2](ClO_4)_2$ (L^1 = pyridine; **1**, 4-picoline; **2**, 4-*tert*-butylpyridine; **3**, *N*-methylimidazole; **4**)[54] was obtained, (ii) We also managed to exchange counter anions by using $[Mn_2(saltmen)_2(H_2O)_2](A)_2$ ($A^- = BF_4^-$, PF_6^-) and $Mn_2(saltmen)_2(ReO_4)_2$ starting materials in reactions with $Ni(pao)_2(py)_2$: $[Mn_2(saltmen)_2Ni(pao)_2(py)_2](A)_2$ (A = BF_4^-; **5**, PF_6^-; **6**, ReO_4^-; **7**)[54] (Fig. 10b). The $[Mn_2(saltmen)_2Ni(pao)_2(L)_2](A)_2$ series of compounds was synthesized in a methanol/water medium by the direct reaction of adequate building blocks in a molar ratio of 1:2, i.e., one equivalent of Mn dimer for two equivalents of Ni building-block (i.e., a Mn:Ni = 1:1 ratio). The yield of the final products was not improved by changing the Mn:Ni reaction ratio. Although an equilibrium between the monomeric $[Mn(saltmen)]^+$ and dimeric $[Mn_2(saltmen)_2]^{2+}$ species generally occurs in methanol/water media, this result indicates that the $Ni(pao)_2(L^1)_2$ monomer reacts selectively with the $[Mn_2(saltmen)_2]^{2+}$ dimer in these reaction conditions. The origin of this selectivity has not been clearly identified, but it could be due to a coordination affinity of the Ni^{II} *donor* building blocks and also to packing effects of the final materials.

Compounds **1**, **4**, **6**, and **7** crystallized in the same monoclinic space group, $C2/c$ (#15), and are isostructural (Fig. 17 and 18). These compounds are composed of $Ni^{II}(pao)_2(L^1)_2$

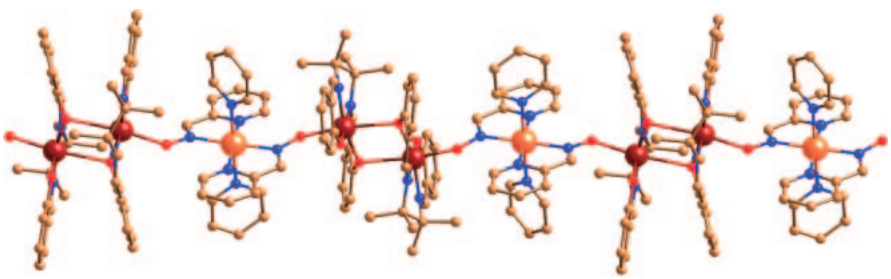

Fig. 17. One-dimensional topology of **1**.

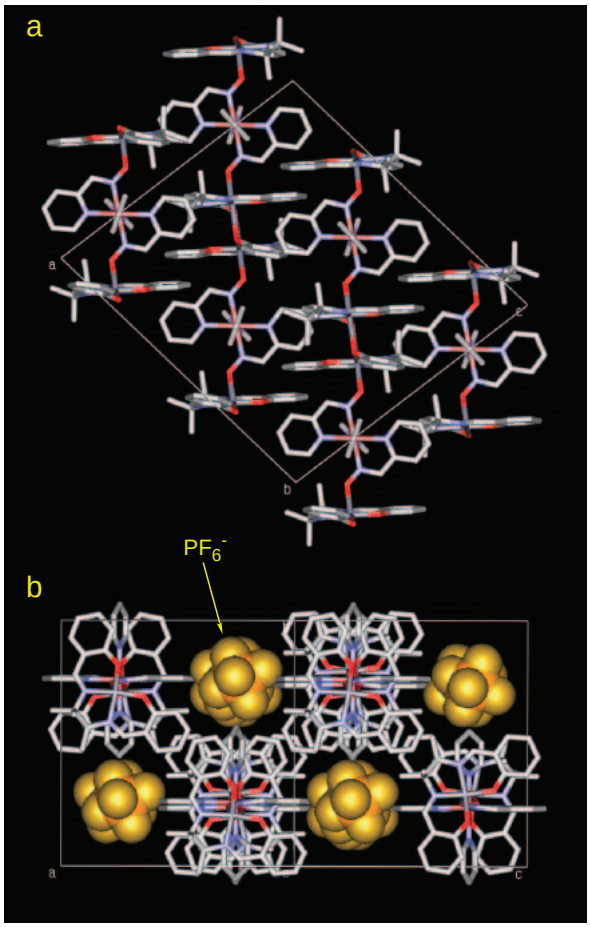

Fig. 18. Packing diagram of **6** showing (a) the projection in the *ac* plane where the chains are running in the $(a + c)$ direction (PF_6^- counter ions located between chains and hydrogen atoms are omitted for clarity) and (b) the projection along the chain axis. (Reprinted with permission from Ref. 54. Copyright 2003, The American Chemical Society).

and Mn^{III}/saltmen dimer units that form an alternating one-dimensional chain with a repeating unit of [–Mn^{III}–ON–Ni^{II}–NO–Mn^{III}–$(O_{ph})_2$–] (Fig. 17 and see discussion in Section **5**).

The Ni^{II} center has a two-fold axis and the out-of-plane dimer, $[Mn_2(saltmen)_2]$, lies on an inversion center. The asymmetric unit thus contains only one Mn^{III} moiety and half of a Ni^{II} pao unit. These symmetry arguments simplify the system considerably and the interpretation of the magnetic properties as well. Indeed, the symmetry implies only one kind of bridge between Mn^{III} and Ni^{II} ions and between Mn^{III} ions. Therefore only two exchange magnetic interactions become necessary to describe the system (vide infra). In term of bond distances and angles, the NO bridge between Mn^{III} and Ni^{II} ions is almost identical along all the structurally characterized compounds (Table 4). The out-of-plane dimer, $[Mn_2(saltmen)_2]$, assumes a square bipyramidal six-coordination geometry with a Jahn–Teller distortion orientated along the chain direction (Fig. 3b). As expected for this type of distortion, longer bond distances (see Table 4) are found in the axial position occupied by the phenolate oxygen O(1*) arising from neighboring $[Mn(saltmen)]^+$ moiety forming an out-of-plane dimer [Mn–O(1*) = 2.470(5)–2.537(3) Å] and by oximato oxygen O(3) arising from $Ni(pao)_2(L^1)_2$ moiety [Mn–O(3) = 2.100(3)–2.122(5) Å] (equatorial average bond distances: ⟨Mn–N⟩ = 1.989 Å and ⟨Mn–O⟩ = 1.893 Å).

As an illustration of the general packing diagram in these compounds, Figure 18 shows two projection views of **6**. Each chain runs in the *ac* plane along the $(a + c)$ direction (Fig. 18a), and counter anions are evenly located between chains (Fig. 18b). Thereby, each chain is separated from the nearest chains with a minimum inter-metallic distance between Mn and Ni ions of 10.39 Å for **1**, 10.36 Å for **4**, 10.51 Å for **6**, and 10.30 Å for **7**. Thus, this counter-anion arrangement plays clearly a key role in the magnetic isolation of the chains. It is also important to note for the magnetic discussion that no significant inter-chain weak interaction, such as interchain π–π stacking between phenyl rings of the saltmen ligands or hydrogen bonding, is observed in **1**, **4**, **6**, and **7**. X-ray diffraction analyses on powder samples of **2**, **3**, and **5** revealed, in all cases, that they are constructed with similar one-dimensional

Table 4. Important Structural Distances and Magnetic Parameters for One-Dimensional Chain Compounds **1**–**7**[42,54,55]

Compd	Mn–$O_{oximate}$ distance /Å	Mn–O–N angle /°	Mn–$O_{phenolate}$ distance /Å	Mn–O–Mn* angle /°	The nearest interchain M–M distance /Å	Magnetic interactions[a]		Arrhenius parameters	
						J/k_B[b] [K]	J_i/k_B[c] [K]	τ_0/s	Δ/k_B [K]
1	2.116(3)	131.8(2)	2.551(3)	98.9(1)	10.39	−20.8(2)	+0.70(2)	$0.6(1) \times 10^{-10}$	74.0(2)
2						−22.2(2)	+0.71(2)	$0.8(1) \times 10^{-10}$	68.0(2)
3						−24.2(2)	+0.62(2)	$1.3(1) \times 10^{-10}$	68.3(2)
4	2.106(5)	134.9(5)	2.503(6)	99.3(2)	10.36	−22.2(2)	+0.76(2)	$1.0(1) \times 10^{-10}$	70.9(2)
5						−21.4(2)	+0.79(2)	$1.2(1) \times 10^{-10}$	67.6(2)
6	2.100(3)	132.4(3)	2.537(3)	99.5(1)	10.51	−21.5(2)	+0.80(2)	$1.2(1) \times 10^{-10}$	67.8(2)
7	2.122(5)	133.4(5)	2.470(5)	98.8(2)	10.30	−21.2(2)	+0.84(2)	$0.8(1) \times 10^{-10}$	72.6(2)

a) The parameters obtained by best-fitting simulation using the Heisenberg trimer model of [Mn^{III}···Ni^{II}···Mn^{III}] ($S = 2, 1, 2$) with inter-trimer interactions treated in a mean-field approximation in the temperature range of 30 to 300 K (see text), note that the average g value was fixed at 1.99. b) The J/k_B refers to the intratrimer magnetic interaction between Mn^{III} and Ni^{II} ions via oximate bridge. c) Neglecting inter-chain interactions, the J_i/k_B refers directly to the intertrimer magnetic exchange interaction therefore $J_{Mn-Mn} = J_i S_T^2 / S_{Mn}^2$.

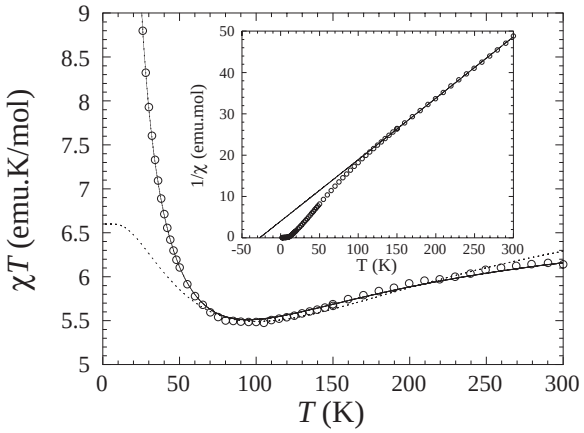

Fig. 19. Temperature dependence of the χT product (where $\chi = M/H$) at 1000 Oe above 30 K measured on a polycrystalline sample of **1**. Dotted and solid lines correspond to the best fits obtained with a trimer $Mn^{III}\cdots Ni^{II}\cdots Mn^{III}$ model and the mean field approximation for a chain of weakly coupled trimers, respectively. Inset: Temperature dependence of the $1/\chi$ at 1000 Oe between 1.8 and 300 K. Solid line corresponds to the best fit obtained with the Curie–Weiss law above 120 K (Reprinted with permission from Ref. 42. Copyright 2002, The American Chemical Society).

arrangements.[54]

Figure 19 shows the temperature dependence of χT for **1** as a typical set of data among the series. With decreasing temperature, the χT product decreases gradually and shows a minimum around 100 K. Below this temperature, χT increases abruptly to reach a maximum of around 6 K ($\chi T_{max} = 80$–$100\,cm^3\cdot K\cdot mol^{-1}$ at 6–7 K, depending on the compounds), and finally decreases again at lower temperatures. The decrease of χT above 100 K is well understood by the antiferromagnetic interaction between Mn^{III} ions and Ni^{II} ions via the oximate bridge already observed in the trinuclear and tetranuclear compounds (Sections **5** and **4**).[20,53] However, the abrupt increase of χT below 100 K is not seen in the trinuclear complexes and reveals the presence of weak ferromagnetic interactions, as expected between Mn^{III} ions via the phenolate bridge. It is noteworthy at this point that the direct observation of ferromagnetic exchange on the χT vs T plot indicates that ferromagnetic $Mn^{III}\cdots Mn^{III}$ interaction clearly overcomes the inter-chain antiferromagnetic ones.[73] Therefore, the material looks like an assembly of trimers [$Mn^{III}\cdots Ni^{II}\cdots Mn^{III}$] with relatively strong $Ni^{II}\cdots Mn^{III}$ antiferromagnetic interaction (J) connected through weak ferromagnetic interactions between the trimers (J').

From this viewpoint, the magnetic susceptibility of this system can be modeled by the simple Mn^{III}–Ni^{II}–Mn^{III} trimer model ($S_{Mn} = 2$, $S_{Ni} = 1$), based on the Heisenberg Hamiltonian (Eq. 1, Section **5**). Nevertheless, ferromagnetic inter-trimer magnetic couplings (J') along the chain need to be considered to reproduce the χT increase below 100 K. As mentioned above, these interactions are significantly weaker than the intra-trimer Ni^{II}–Mn^{III} coupling. Therefore, this magnetic coupling has been treated in a mean field approximation (MFA):[72]

$$\chi = \frac{\chi_{trimer}}{1 - \dfrac{4J_i}{Ng^2\mu_B^2}\chi_{trimer}}, \qquad (2')$$

where J_i is the sum of the magnetic interactions around each trimer which is surrounded by two trimers within a chain and by eight trimers on neighboring chains (see Fig. 18), therefore $J_i = J' + 4J''$, where J'' is considered to be the whole inter-chain antiferromagnetic interaction. This model reproduces with a good agreement the experimental data for all compounds above 30 K (the simulation curve for **1** is shown in Fig. 19, solid line; the best sets of parameters for **1**–**7** are summarized in Table 4). It should be mentioned that the calculated parameters are in good agreement with those obtained in the primary and secondary building units (vide supra). As expected from the structural description of **1**, **4**, **6**, and **7**, magnetic parameters are very similar among the series and no clear correlation with structural distances and angles has been observed. Based on Eq. 2′ and considering isotropic interactions ($J' \approx |J''|$), a divergence of the susceptibility is predicted at low temperatures, for example at $T_{MF} = 10.7$ K for **1** as shown in Fig. 20. However, this behavior is not observed experimentally and a large deviation from the MFA is found at low temperatures (see Fig. 20). This result emphasizes the anisotropy of the inter-trimer interactions ($J' \gg |J''|$ and then $J' \approx J_i$) and the one-dimensional nature of the system.

To discuss in more details the anisotropic nature of these one-dimensional compounds, we have performed experiments on oriented single crystals. The susceptibility has been measured in three perpendicular directions including the monoclinic b axis (Figure 21 gives the data for **1**). Below 60 K, the susceptibility becomes strongly anisotropic and reveals a quasi uni-axial symmetry above 20 K.[74] These results clearly establish the position of the easy axis along the chain direction in agreement with the alignment of the local Jahn–Teller axis on Mn^{III} ion along the chain. This anisotropy is confirmed

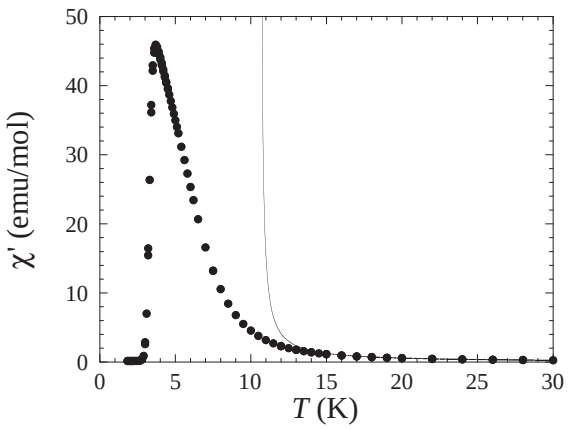

Fig. 20. Temperature dependence of the susceptibility χ' (where $\chi' = dM/dH$) on a polycrystalline sample of **1** at zero dc magnetic field and a 3 Oe ac field, at 1 Hz from 1.8 to 7 K and at 125 Hz above 7 K, where χ' is independent of the ac frequency above 3.5 K (peak temperature). Solid line is the mean field fit shown in Fig. 19 (Reprinted with permission from Ref. 42. Copyright 2002, The American Chemical Society).

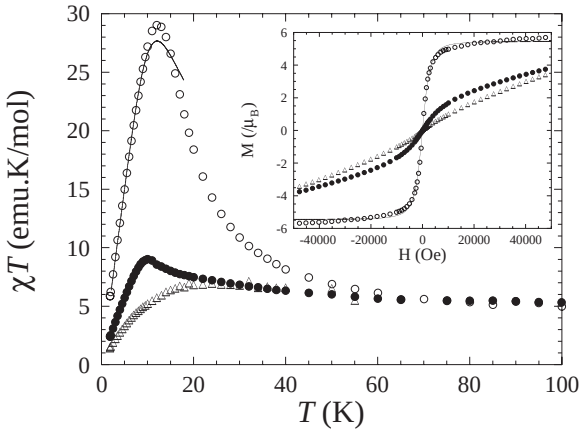

Fig. 21. Magnetic measurements on oriented single crystals of **1** along the chains (○), perpendicular to the chains in the (*ac*) plane (●), and along the monoclinic *b* axis (△), respectively. Temperature dependence of the χT product (where $\chi = M/H$) at 10 kOe below 100 K, the solid line corresponds to the best fits obtained with the 1-D Ising model. Inset: Field dependence of the magnetization at 10 K. Solid line corresponds to the best fit obtained with the 1-D Ising model (Reprinted with permission from Ref. 42. Copyright 2002, The American Chemical Society).

by the field dependence of the magnetization (for example for **1** at 10 K, inset of Fig. 21). The magnetization quickly saturates when the field is applied along the chain direction, at $6\mu_B$ per trimer (expected value for the $S_T = 3$ spin ground state arisen from an antiferromagnetically-coupled Mn^{III}···Ni^{II}···Mn^{III} trimer). This low temperature behavior has been simulated using a one-dimensional Ising model. For that, we have used a simplified treatment which consists in keeping only the two $S_{Tz} = \pm 3$ spin states.[75] At this approximation, the Hamiltonian reads:

$$H = -2J' \sum_i S_{Tzi} \cdot S_{Tz(i+1)} + g\mu_B H_z \sum_i S_{Tzi}. \quad (3)$$

To identify this expression with the 1-D Ising Hamiltonian, one should introduce $\sigma_i = -S_{Tzi}/3$ (with $\sigma_i = \pm 1$). Therefore using the Glauber notation,[36] Eq. 3 becomes:

$$H = -J'_{eff} \sum_i \sigma_i \sigma_{i+1} - \mu_{eff} H \sum_i \sigma_i, \quad (4)$$

with $J'_{eff} = 18J'$ and $\mu_{eff} = 3g\mu_B \approx 6\mu_B$.[76] This model gives the magnetization as functions of the temperature and the magnetic field:

$$M = N\mu_{eff} \frac{\sinh\left(\frac{\mu_{eff}H}{k_B T}\right)}{\sqrt{\sinh^2\left(\frac{\mu_{eff}H}{k_B T}\right) + \exp\left(\frac{-4J'_{eff}}{k_B T}\right)}}. \quad (5)$$

This expression has been used to fit the data between 5 and 15 K (solid lines in Fig. 21 and its inset). The obtained parameters are $\mu_{eff}/\mu_B = 5.4$, and $J'_{eff}/k_B = +12$ K. The former value is consistent with the expected moment at saturation $\mu_{eff}/\mu_B = 6$ and the latter gives $J'/k_B = +0.67$ K, in agreement with the value previously estimated from the high temperature magnetic susceptibility (vide supra). It is worth noticing that the rapid saturation of the magnetization along the chain (inset of Fig. 21) is compatible with 1-D correlations and does not imply a long-range magnetic order. Above 15 K, the theoretical model will be more complicated, due to the population of the trimer excited states and to the necessary crossover towards a Heisenberg behavior described previously.

Single-crystal measurements below 3 K have been also carried out by micro-SQUID technique[77] (hysteresis and dc relaxation measurements) and Hall probe magnetometry (transverse field magnetization measurements). When the external field is applied parallel to the chain direction (easy axis) (Fig. 22a),

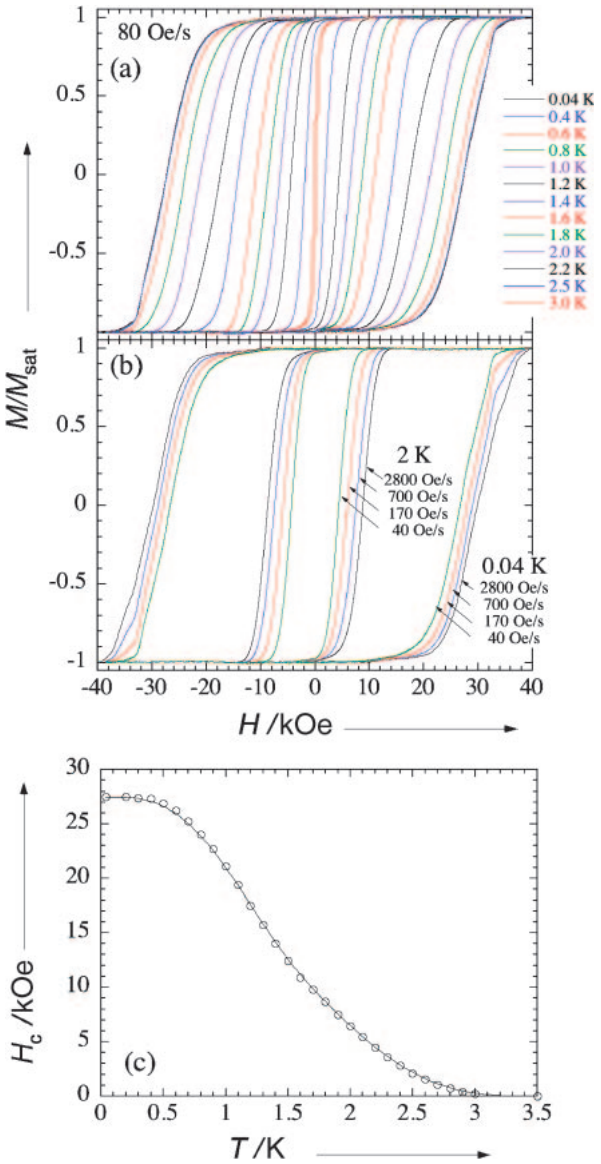

Fig. 22. Measurements on a single crystal of **1** in the easy direction (chain axis). Field dependence of the magnetization (a) at different temperature with 80 Oe/s field sweep rate and (b) at 2 K and 0.04 K at different field sweep rates; (c) Temperature dependence of the coercive field with 80 Oe/s field sweep rate (Reprinted with permission from Ref. 54. Copyright 2003, The American Chemical Society).

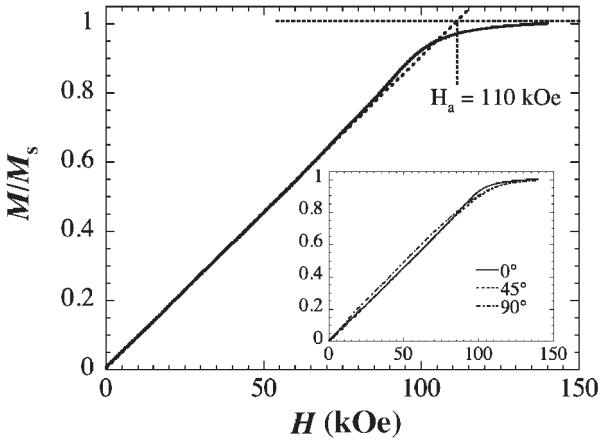

Fig. 23. Field dependence of the magnetization (normalized at the saturation value) of **1** when the magnetic field is applied perpendicular to the easy axis at 1.5 K. The intersection between the two dotted lines gives the anisotropy field. Inset: Similar measurements than the main figure at three angles in the plan normal to the easy axis. The main figure is at $\theta = 0^\circ$ (Reprinted with permission from Ref. 55. Copyright 2004, The American Physical Society).

hysteresis loops are observed below 3 K and the coercive field increases very rapidly with lowering temperature (Figs. 22a and 22c) to reach 2.75 T at 0.4 K. For the whole series of compounds, field dependence of the magnetization below 3.5 K reveals the presence of hysteresis loops confirming the slow relaxation of the magnetization and their "magnet-type" properties, i.e. SCM behavior. On the other hand, when the external field is applied perpendicular to the chain direction (Fig. 23), no hysteresis effect is observed and the same field dependence of the magnetization is obtained independently of the field angle. This result proves clearly the uni-axial anisotropy in these compounds (Ising-type chain), confirming the data obtained from the classical SQUID technique (Fig. 21). Moreover, applying the field in the hard plane leads to a linear increase of the magnetization and to a saturation at 11.0 T. This field corresponds to the anisotropic field H_a which gives us an estimation of the intrinsic finite anisotropy of the $S_T = 3$ trimer unit. From the relation of $2|D|{S_T}^2 = g\mu_B S_T H_a$, we approximately obtained $D/k_B = -2.5$ K for **1**. It is noteworthy that this D value is in excellent agreement with the values estimated for the trinuclear SMM compounds $[Mn_2(5\text{-R-saltmen})_2Ni(pao)_2(phen)](ClO_4)_2$ (R = Cl, Br) ($D/k_B = -2.4$ K, Section **5**).

In order to probe the dynamics of the magnetization in these one-dimensional systems, we have performed ac magnetic susceptibility measurements. For all the one-dimensional compounds reported here, the frequency dependence of ac susceptibilities was measured in the temperature range of 1.8–7 K under an oscillating magnetic field of 1 or 3 Oe and with zero dc magnetic field. Below 6.5 K, χ' and χ'' are strongly frequency dependent along the series of materials (see Fig. 24 for **1**). At a fixed temperature, χ' and χ'' were also measured as a function of ac frequency, ν_{ac}, ranging from 1 to 1500 Hz. From these measurements, Cole–Cole diagrams (χ'' vs χ' plot) with a nearly semi-circle shape have been obtained. These data have been fitted to the generalized Debye model with small distribution coefficient α values (<0.1) indicating a weak distribution of relaxation times (Fig. 25).[78] We have, therefore, considered that the relaxation process of the magnetization is occurring essentially with a single relaxation time. Moreover, slight modifications at the molecular level on the counter anion or on the L^1 ligand have a very weak influence on the ac magnetic behavior, highlighting the one-dimensional nature of the observed magnetic properties. Additionally, the study of the relaxation process and its characteristic time unambiguously precludes possibilities of three-dimensional classical magnets,

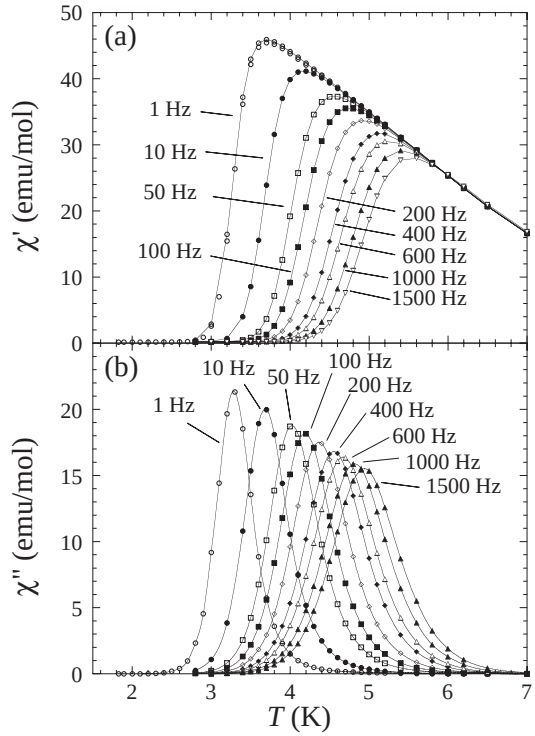

Fig. 24. Temperature and frequency dependence of the (a) real and (b) imaginary part of the ac susceptibility for **1**. Solid lines are guides for the eyes (Reprinted with permission from Ref. 42. Copyright 2002, The American Chemical Society).

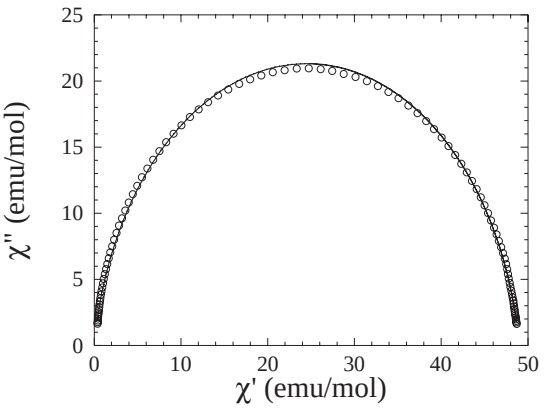

Fig. 25. Cole–Cole diagram at 4 K for **1**. Solid line represent the least-square fit obtained with a Debye model (Reprinted with permission from Ref. 42. Copyright 2002, The American Chemical Society).

superparamagnetic nanoparticles,[79] or spin-glass-like materials.[80–83]

Taking into account that only one relaxation process occurs in these materials, we conclude that the temperature at the maximum of the $\chi''(T)$ curves corresponds to the blocking temperature $T_B(\nu_{ac})$ for a given frequency, ν_{ac}. At T_B, the relaxation time of the system (τ) is equal to the characteristic time of the experiments (τ_{exp}): $\tau(T_B) = \tau_{exp} = 1/(2\pi\nu_{ac})$. The thermal variation of τ is experimentally well described by an Arrhenius law (i.e., thermally activated behavior):

$$\tau(T_B) = \tau_0 \exp\left(\frac{\Delta}{k_B T}\right), \quad (6)$$

where τ_0 is the pre-exponential factor and Δ is the energy barrier to reverse the magnetization direction. At a given T_B, Eq. 6 implies:

$$\ln(\tau) = \ln(\tau_0) + \frac{\Delta}{k_B T_B}, \quad (7)$$

or

$$\frac{1}{T_B} = -\frac{k_B}{\Delta}[\ln(2\pi\nu) + \ln(\tau_0)]. \quad (7')$$

Across the series, the $1/T_B$ vs $\ln(2\pi\nu)$ plots (Fig. 26) have been thus fitted to a linear function to deduce the pre-exponential factors (τ_0) and characteristic energies (Δ). These parameters are very similar across the series: $\tau_0 \approx 1 \times 10^{-10}$ s and $\Delta/k_B \approx 70$ K, as summarized in Table 4.

At this point, we can conclude that the present compounds **1**–**7** are built from magnetically isolated chains of ferromagnetically-coupled uni-axial $S_T = 3$ units with $J'/k_B \approx +0.8$ K and $D/k_B \approx -2.5$ K (Fig. 12), exhibiting slow relaxation of the magnetization. The dynamics of the magnetization have been probed by ac susceptibility measurements and a thermally activated single relaxation time has been found. It should be emphasized here that combined dc and ac measurements on powder and single-crystal measurements down to very low temperatures (40 mK) are all essential to prove what we call "SCM behavior."

Even if we have experimentally and clearly established the SCM behavior in these systems, the interpretation of the magnetic parameters, mainly of their energy barrier, is still lacking at this stage. The next questions are now naturally: (i) Can we use the Glauber theory developed 40 years ago for chains of ferromagnetically-coupled Ising spins in our real systems? (ii) Can we understand why the energy gap, Δ, of our SCM system (~70 K) is completely different from the one observed for the trinuclear unit of $[Mn_2(5\text{-R-saltmen})_2Ni(pao)_2(phen)](ClO_4)_2$ (R = Cl, Br) (~18 K) in spite of their similar S_T and $D_{S_T=3}$? (iii) What is the role of the intra-chain magnetic interaction (J') and the finite anisotropy (D)? These are the main questions that we will try to answer in the following section.

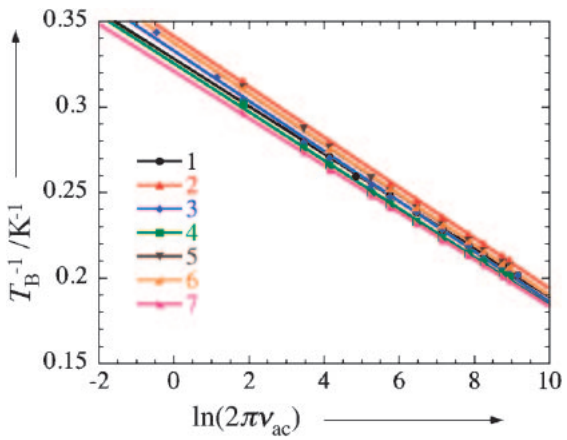

Fig. 26. $1/T_B$ versus $\ln(2\pi\nu_{ac})$ plots. The solid lines represent the least-square linear fits of the experimental data with the Arrhenius equation (Reprinted with permission from Ref. 54. Copyright 2003, The American Chemical Society).

7. Slow Relaxation of the Magnetization in Single-Chain Magnets

As illustrated by the experimental results obtained on the family of SCM materials $[Mn_2(saltmen)_2Ni(pao)_2(L^1)_2](A)_2$ and summarized in Section **6**, the slow relaxation of the magnetization is not solely the consequence of the uni-axial anisotropy (D) seen by each spin (or unit spin) on the chain but depends also on magnetic correlations (J'). In one-dimensional systems, the effect of the short-range order becomes more and more important when the temperature is reduced, until a critical point is reached at $T = 0$ K. In fact, the experimental relaxation time (Fig. 26) is found to be exponentially enhanced at low temperatures, in agreement with the pioneer work of Glauber devoted to chains of ferromagnetically-coupled Ising spins and their dynamics.[36] According to Glauber theory,[84] the relaxation time follows an activated law:

$$\tau(T) = \tau_i(T) \exp\left(\frac{8J'S_T^2}{k_B T}\right), \quad (8)$$

where the pre-exponential factor τ_i introduced phenomenologically by Glauber describes the individual dynamics of the spin unit composing a chain, and therefore, generally depends on temperature.[36] In Eq. 8, the exponential factor is directly related to the temperature dependence of the correlation functions. In the case of a finite uni-axial anisotropy, D, the correlation length remains exponentially enhanced at low temperatures and we can still expect a thermally activated relaxation.[85] The value of the corresponding gap remains the same as in the Ising limit as long as $|D| \geq 4J'/3$.[86] Indeed, the $[Mn_2(saltmen)_2Ni(pao)_2(L^1)_2](A)_2$ materials fall in this limit based on $J'/k_B \approx +0.8$ K and $D/k_B \approx -2.5$ K (Section **6**) and thus Eq. 8 remains valid. In the simple case of anisotropic isolated units ($J' = 0$), i.e. the SMM case, we expect that τ_i follows an activated law:

$$\tau_i(T) = \tau_0 \exp\left(\frac{|D|S_T^2}{k_B T}\right), \quad (9)$$

where D is the single unit anisotropy taken negative for uni-axial case, and τ_0 is a pre-exponential factor characteristic of the system. As shown in Sections **2** and **5**, this thermally activated behavior is experimentally observed when the quantum tunneling of the magnetization[87,88] can be ignored. In the case of the anisotropic units coupled ferromagnetically along a chain, i.e. ferromagnetic SCMs, the relaxation time is hence expected to follow an activated behavior:

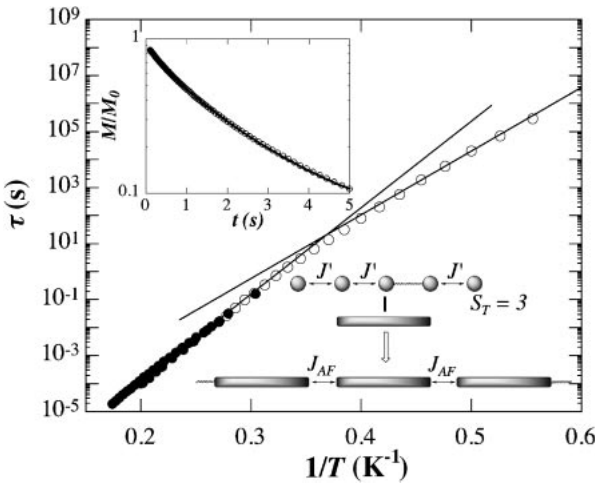

Fig. 27. Semilog plot of the relaxation time τ vs $1/T$ for **1**. The full and open dots were obtained from ac and dc measurements, respectively. The corresponding straight lines give the energy gap: $\Delta_1/k_B \approx 74$ K and $\Delta_2/k_B \approx 55$ K. Inset: Relaxation of the magnetization at 3 K (top). Schematic view of the magnetic interactions for the model (bottom) (Adapted from Ref. 55. Copyright 2004, The American Physical Society).

$$\tau(T) = \tau_0 \exp\left[\frac{(8J' + |D|){S_T}^2}{k_B T}\right], \tag{10}$$

where $(8J' + |D|){S_T}^2$ corresponds to the energy barrier to reverse the magnetization direction (based on the Hamiltonian given by Eq. 3). As shown in Fig. 27, combined ac and dc measurements have allowed us to estimate the relaxation time for **1** on an extended range of temperature 7 to 1.8 K.[55] Two activated regimes are found, above and below 2.7 K, with two energy barriers: $\Delta_1/k_B \approx 74$ K and $\Delta_2/k_B \approx 55$ K. Based on the magnetic parameters (J', D, and S_T) evaluated for **1** in Section **6** ($J'/k_B = +0.7$ K, $D/k_B = -2.5$ K and $S_T = 3$), the energy barrier deduced from the Glauber theory, $\Delta_{Glauber} = (8J' + |D|){S_T}^2$, is equal to ca. 73 K in excellent agreement with the value experimentally obtained above 2.7 K: $\Delta_1/k_B \approx 74$ K.

Indeed, we realized that the influence of defects in the chain had to be considered in order to understand the low temperature regime of the relaxation (below 2.7 K). As the magnetic correlation length of the infinite chain, ξ, becomes exponentially large at low temperatures, even a very small number of defects can deeply affect the relaxation process. These defects limit the size of the chain and therefore a finite-size scaling of the Glauber model has to be considered to calculate the relaxation time in this regime.[89] Following the model developed in Ref. 89b when ξ becomes larger than the chain length, L, the relaxation time energy barrier becomes $(4J' + |D|){S_T}^2$ ($\sim$48 K),[55] in remarkable agreement with the experimental value $\Delta_2/k_B \approx 55$ K. Hence for the first time, this study shows that two relaxation regimes that should be systematically observed in *Single-Chain Magnets*. At high temperature, the one-dimensional assembly behaves as an infinite chain and the relaxation time follows the Glauber theory, which need to be generalized for finite anisotropy in real systems: the energy barrier is then $\Delta_{Glauber} = (8J' + |D|){S_T}^2$. At low temperatures below a crossover temperature (ca. 2.7 K in **1**), a second activated regime is found when the correlation length becomes larger than the intrinsic chain length of the compound: the energy barrier becomes then $(4J' + |D|){S_T}^2$.

It should be noted that this crossover is induced by intrinsic defects on the chain, which limit the growth of the 1-D correlations. Therefore, as in any classical problem, here χT is proportional to ξ,[90] so a crossover should also be found on the magnetic susceptibility. In a ferromagnetic one-dimensional anisotropic Heisenberg model, this correlation length is exponentially enhanced for any value of D when lowering the temperature. In the $|D| > 4J'/3$ Ising limit, the susceptibility is given by:[85]

$$\chi_\infty = \frac{C_{eff}}{T} \exp\left(\frac{4J'{S_T}^2}{k_B T}\right), \tag{11}$$

therefore:

$$\ln(\chi_\infty T) = \ln(C_{eff}) + \frac{4J'{S_T}^2}{k_B T}, \tag{11'}$$

where C_{eff} is the effective Curie constant of the chain.[55] As expected at high temperature, Figure 28 shows for **1** that $\ln(\chi T)$ vs $1/T$ increases linearly with an energy gap of 28 K. This energy gap allows an estimation of $J'/k_B = +0.78$ K, in good agreement with the value (+0.7 K) estimated in the fitting of the χT vs T plot using the mean-field approximation (Fig. 19 and Table 4).

When the correlation length becomes larger than the real chain length (L), the χT product qualitatively saturates at about 200 $cm^3 \cdot K \cdot mol^{-1}$. In this limit, the value of saturation is simply equal to nC_{eff} where C_{eff} and n are the effective Curie constant of the chain defined previously ($C_{eff} = 2.7$ $cm^3 \cdot K \cdot mol^{-1}$) and the number of units in the chain, respectively. Therefore, n can be roughly estimated at around 75 and then the chain length is about 105 nm for **1**. Nevertheless, the slight decrease of χT from the saturated value is mainly due to weak antiferromagnetic interaction functioning between finite chains of n spins (inset Fig. 27). Therefore, a complete model of antiferromagnetically-coupled finite-size chains has been developed to fit the experimental data in the low field approximation (solid line Fig. 28):[55]

$$\chi = \frac{C_{eff}}{T} \exp\left(\frac{4J'{S_T}^2}{k_B T}\right) \left\{ 1 - \frac{\left(1 - \exp\left(-2n \exp\left(-\frac{4J'{S_T}^2}{k_B T}\right)\right)\right)\left(1 - \tanh\left(\frac{2J_{AF}{S_T}^2}{k_B T}\right)\right)}{2n \exp\left(-\frac{4J'{S_T}^2}{k_B T}\right)\left(1 - \tanh\left(\frac{2J_{AF}{S_T}^2}{k_B T}\right) \exp\left(-2n \exp\left(-\frac{4J'{S_T}^2}{k_B T}\right)\right)\right)} \right\}. \tag{12}$$

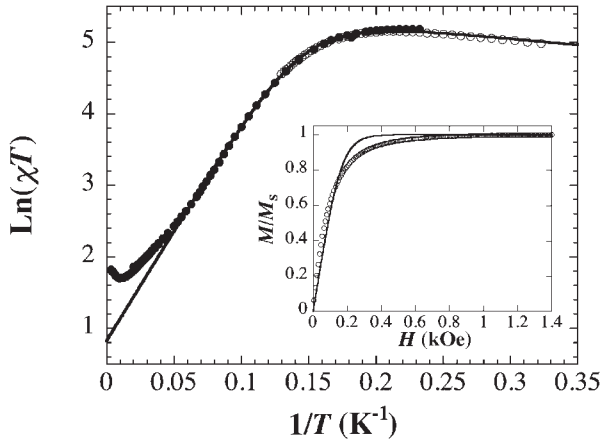

Fig. 28. Semilog plot of χT vs $1/T$ (χ is given in emu·mol^{-1}) for **1**. The full and open dots were obtained from ac and dc measurements, respectively. Inset: Field dependence of the magnetization (normalized at saturation value) at 4 K and with a field sweep rate of 0.14 kOe·s^{-1}. Solid lines correspond to the fit using the expressions of given in Ref. 55 (Reprinted with permission from Ref. 55. Copyright The American Physical Society).

Using this model for **1**, we found $J'/k_B \approx +0.78$ K and $J_{AF}/k_B \approx -0.047$ K,[91] and the average number of spins between two defects $n \approx 110$, which corresponds to an average chain length of $L \approx 140$ nm. As shown in the inset of Fig. 28, we also modeled the magnetization as a function of the applied field[55] and we obtained $n \approx 90$ in relatively good agreement with the value deduced from the susceptibility.

In this section, we have shown that the *Single-Chain Magnet* behavior, its associated relaxation time and magnetic susceptibility can be perfectly understood in the frame of the Glauber theory adapted with a finite anisotropy and taking into account finite-size effects. The simultaneous interpretation of both τ and χ allows us to deduce all the parameters ($\Delta_{Glauber}$ or Δ_1, Δ_2, J', J_{AF}, and n) of the system. The activation energies of a SCM is thus a combined effect of: (i) the individual kinetics of unit composing the chain and (ii) the one-dimensional magnetic correlations.

Concluding Remarks

Only in 2001 and almost forty years after the pioneering work of R. J. Glauber on the dynamics of ferromagnetic Ising chains,[36] the first experimental evidence of the magnetization slow relaxation in a one-dimensional object has been reported by Gatteschi and co-workers.[40a] One year later, we have reported what is still to date the simplest one-dimensional system to probe the Glauber theory.[42] Indeed, the $[Mn_2(saltmen)_2Ni(pao)_2(L^1)_2]_n^{2n+}$ chains are very similar to the prototype of the Glauber chains as they can be viewed as one-dimensional arrangements of perfectly aligned ferromagnetically-coupled anisotropic $S_T = 3$ spin units. In this review, we have presented our synthetic strategy to built series of one-dimensional magnets or what we have called *Single-Chain Magnets* (SCMs). Using a step-by-step approach with complementary and functionalized building blocks (with a *trans*-bicoordination ability, a good steric hindrance, and a large uniaxial anisotropy), we have been able (i) to synthesize premeditated SCM systems easily modified at the molecular level and therefore (ii) to probe systematically the SCM properties. In this synthetic quest, we have also isolated oligomers (di-, tri-, and tetra-nuclear complexes)[14,20,53,58] that indeed exhibit interesting magnetic properties such as SMM behavior, but also have helped us to determine and verify the magnetic characteristic (D, J_{Mn-Mn}, J_{Mn-Ni}, and g) of our final chain compounds. Among these species, trinuclear $[Mn_2(5\text{-R-saltmen})_2Ni(pao)_2(phen)]^{2+}$ (R = Cl, Br) complexes are SMMs and also the repeating units of the SCM family of $[Mn_2(saltmen)_2Ni(pao)_2(L^1)_2]_n^{2n+}$ could be SMMs. This result demonstrates for the first time that the synthesis of SCMs can be achieved by connecting ferromagnetically SMMs in one-dimension. This idea is also underlying the conclusions given by the analysis of the SCM behavior (Section **7**). Indeed, the relaxation of the magnetization is thermally activated in both SMM and SCM, but the energy barrier changes from $\Delta_{SMM} = |D|S_T^2$ (when quantum tunneling of the magnetization is negligible) to $\Delta_{SCM} = (8J' + |D|)S_T^2$ (in the infinite chain limit and if $|D| \geq 4J'/3$), showing the effect of the one-dimensional correlation. In other words, SMMs are a limit case of SCM when $J' = 0$. In 2002, Wernsdorfer and co-workers have also discussed the effects of magnetic interaction between SMMs.[27] They have shown in a H-bonded dimer of SMM that the inter-SMM's interaction enables to tune the quantum tunneling of the magnetization. This breakthrough opens new perspectives in the field of molecule-based magnetism to introduce magnetic interactions between SMM clusters in 1-D, 2-D, and 3-D architectures.[92] If quantum effects can be seen on a dimer of SMM, the next step would be naturally to discuss possible quantum effects in SCM. Following this idea, it is interesting to note on Fig. 22c that, below 0.4 K, the hysteresis loop observed in the easy direction of **1** becomes temperature independent at a given field sweep rate. Similar behavior can be seen in SMM systems at very low temperatures, when the dynamics is dominated by quantum tunneling of the magnetization (see for example Fig. 8). Unfortunately, in our one-dimensional systems, the relaxation time becomes too slow to be measured using dc or ac techniques. Nevertheless, this result suggests that a quantum tunneling effect might exist at low temperatures (here below 0.4 K in **1**) in our SCM system as another relaxation regime. Indeed such conclusions have already been proposed in recent papers;[43d,93] even so, a detailed study and analysis of this regime still needs to be carried out in order to prove unambiguously the relevance of the quantum effects in SCM systems.

In this review, we have also summarized the magnetic signatures of a real SCM system in the Ising limit ($|D| \geq 4J'/3$). We have shown that finite anisotropy and also finite-size chain effects must be included in the Glauber model in order to understand the crossover between two activated regimes of magnetic relaxation observed in SCMs. At high temperatures, the chains can be considered as infinite with an energy barrier of $\Delta = (8J' + |D|)S_T^2$; while at low temperature, the defects along the chain become relevant. The finite length of chains induces thus a decrease of the energy gap to $\Delta = (4J' + |D|)S_T^2$. In parallel to the interpretation of the relaxation time, the magnetic susceptibility confirms this crossover and can be modeled

over the whole range of temperature. From this analysis, the chain length and the magnetic interactions between these finite chains can be estimated. Even if the whole picture seems to be consistent, the crossover is not observed exactly at the same temperature on the relaxation time and the magnetic susceptibility. Hence, additional ingredients such as poly-dispersity on the chain length or exchange interactions may be relevant to improve the discussion of the physical properties of these SCM systems.[55,94]

In the field of molecule-based magnetism, SCMs have become one of the main research trends in only a few years. This subject offers interesting challenges for chemists to design premeditated one-dimensional architectures but also for physicists to understand the one-dimensional slow relaxation of the magnetization and its mechanism. Among them, the influence of the quantum effects is still an open question. *Single-Chain Magnets* are new fascinating materials at the frontier between quantum and classical physics. The compounds reported in this review illustrate how today's chemistry can control the molecular and nano-metric scales in order to build premeditated functional materials in the world of nanotechnologies.

The authors gratefully acknowledge Prof. Claude Coulon of the Centre de Recherche Paul Pascal-CNRS at Pessac in France, Prof. Wolfgang Wernsdorfer of the Laboratoire Louis Néel-CNRS at Grenoble in France, and Prof. Masahiro Yamashita of the Tohoku University at Sendai in Japan for their fruitful collaborations and the hours of helpful and passionate discussions. The authors also thank our students and post-docs at TMU and CRPP for their everyday hard work, but also for their curiosity, enthusiasm, and ability on this project, which have stimulated our own motivation and creativity.

H. M. thanks PRESTO, JST, CREST, JST, and a Grant-in-Aid for Scientific Research from the Ministry of Education, Culture, Sports, Science and Technology, Japan for financial support. R. C. would like to thank the CNRS, the University of Bordeaux 1 and the Conseil Régional d'Aquitaine for financial support.

References

1 E. Coronado, F. Palacio, and J. Veciana, *Angew. Chem., Int. Ed.*, **42**, 2570 (2003).

2 S. K. Ritter, *Chem. Eng. News*, **82**, 29 (2004).

3 G. Christou, D. Gatteschi, D. N. Hendrickson, and R. Sessoli, *MRS Bull.*, **25**, 66 (2000).

4 D. Gatteschi and R. Sessoli, *Angew. Chem., Int. Ed.*, **42**, 268 (2003).

5 D. Gatteschi, A. Caneschi, L. Pardi, and R. Sessoli, *Science*, **265**, 1054 (1994).

6 W. Wernsdorfer and R. Sessoli, *Science*, **284**, 133 (1999).

7 M. N. Leuenberger and D. Loss, *Nature*, **410**, 789 (2001).

8 M. Clemente-León, E. Coronado, A. Forment-Aliaga, and F. M. Romero, *C. R. Chimie*, **6**, 283 (2003).

9 M. Clemente-León, E. Coronado, A. Forment-Aliaga, P. Amorós, J. Ramírez-Castellanos, and J. M. González-Calbet, *J. Mater. Chem.*, **13**, 3089 (2003).

10 A. Cornia, A. C. Fabretti, M. Pacchioni, L. Zobbi, D. Bonacchi, A. Caneschi, D. Gatteschi, R. Biagi, U. Del Pennino, V. De Renzi, L. Gurevich, and H. S. J. Van der Zant, *Angew. Chem., Int. Ed.*, **42**, 1645 (2003).

11 A. Cornia, A. C. Fabretti, M. Pacchioni, L. Zobbi, D. Bonacchi, A. Caneschi, D. Gatteschi, R. Biagi, U. Del Pennino, V. De Renzi, L. Gurevich, and H. S. J. Van der Zant, *J. Magn. Magn. Mater.*, **272–276**, e725 (2004).

12 a) P. D. W. Boyd, Q. Li, J. B. Vincent, K. Folting, H.-R. Chang, W. E. Streib, J. C. Huffman, G. Christou, and D. N. Hendrickson, *J. Am. Chem. Soc.*, **110**, 8537 (1988). b) A. Caneschi, D. Gatteschi, and R. Sessoli, *J. Am. Chem. Soc.*, **113**, 5873 (1991). c) R. Sessoli, H.-L. Tsai, A. R. Schake, S. Wang, J. B. Vincent, K. Folting, D. Gatteschi, G. Christou, and D. N. Hendrickson, *J. Am. Chem. Soc.*, **115**, 1804 (1993). d) H. J. Eppley, H.-L. Tsai, N. de Vries, K. Folting, G. Christou, and D. N. Hendrickson, *J. Am. Chem. Soc.*, **117**, 301 (1995). e) G. Aromi, S. M. J. Aubin, M. A. Bolcar, G. Christou, H. J. Eppley, K. Folting, D. N. Hendrickson, J. C. Huffman, R. C. Squire, H.-L. Tsai, S. Wang, and M. W. Temple, *Polyhedron*, **17**, 3005 (1998). f) S. M. J. Aubin, Z. Sun, L. Pardi, J. Krzystek, K. Folting, L.-C. Brunel, A. L. Rheingold, G. Christou, and D. N. Hendrickson, *Inorg. Chem.*, **38**, 5329 (1999). g) J. C. Goodwin, R. Sessoli, D. Gatteschi, W. Wernsdorfer, A. K. Powell, and S. L. Heath, *J. Chem. Soc., Dalton Trans.*, **2000**, 1835. h) H.-L. Tsai, T.-Y. Jwo, G.-H. Lee, and Y. Wang, *Chem. Lett.*, **2000**, 346. i) S. M. J. Aubin, Z. Sun, H. J. Eppley, E. M. Rumberger, I. A. Guzei, K. Folting, P. K. Gantzel, A. L. Rheingold, G. Christou, and D. N. Hendrickson, *Inorg. Chem.*, **40**, 2127 (2001). j) C.-D. Park, W. Rhee, Y. Kim, W. Jeon, D.-Y. Jung, D. Kim, Y. Do, and H.-C. Ri, *Bull. Korean Chem. Soc.*, **22**, 453 (2001). k) E. Coronado, M. Feliz, A. Forment-Aliaga, C. J. Gómez-García, R. Liusar, and F. M. Romero, *Inorg. Chem.*, **40**, 6084 (2001). l) T. Kuroda-Sowa, M. Lam, A. L. Rheingold, C. Frommen, W. M. Reiff, M. Nakano, J. Yoo, A. L. Maniero, L.-C. Brunel, G. Christou, and D. N. Hendrickson, *Inorg. Chem.*, **40**, 6469 (2001). m) T. Kuroda-Sowa, T. Fukuda, S. Miyoshi, M. Maekawa, M. Munakata, H. Miyasaka, and M. Yamashita, *Chem. Lett.*, **7**, 682 (2002). n) A. Cornia, A. C. Fabretti, R. Sessoli, L. Sorace, D. Gatteschi, A.-L. Barra, C. Daiguebonne, and T. Roisnel, *Acta Crystallogr., Sect. C*, **58**, m371 (2002). o) M. Soler, W. Wernsdorfer, Z. Sun, J. C. Huffman, D. N. Hendrickson, and G. Christou, *Chem. Commun.*, **2003**, 2672. p) M. Soler, W. Wernsdorfer, K. A. Abboud, J. C. Huffman, E. R. Davidson, D. N. Hendrickson, and G. Christou, *J. Am. Chem. Soc.*, **125**, 3576 (2003). q) T. Kuroda-Sowa, T. Nogami, H. Konaka, M. Maekawa, M. Munakata, H. Miyasaka, and M. Yamashita, *Polyhedron*, **22**, 1795 (2003). r) A. Forment-Aliaga, E. Coronado, M. Feliz, A. Gaita-Ariño, R. Llusar, and F. M. Romero, *Inorg. Chem.*, **42**, 8019 (2003). s) H. Zhao, C. P. Berlinguette, J. Bacsa, A. V. Prosvirin, J. K. Bera, S. E. Tichy, E. J. Schelter, and K. R. Dunbar, *Inorg. Chem.*, **43**, 1359 (2004). t) M. Pacchioni, A. Cornia, A. C. Fabretti, L. Zobbi, D. Bonacchi, A. Caneschi, G. Chastanet, D. Gatteschi, and R. Sessoli, *Chem. Commun.*, **2004**, 2604.

13 a) S. M. J. Aubin, M. W. Wemple, D. M. Adams, H.-L. Tsai, G. Christou, and D. N. Hendrickson, *J. Am. Chem. Soc.*, **118**, 7746 (1996). b) J. Yoo, E. K. Brechin, A. Yamaguchi, M. Nakano, J. C. Huffman, A. L. Maniero, L.-C. Brunel, K. Awaga, H. Ishimoto, G. Christou, and D. N. Hendrickson, *Inorg. Chem.*, **39**, 3615 (2000). c) J. Yoo, A. Yamaguchi, M. Nakano, J. Krzystek, W. E. Streib, L.-C. Brunel, H. Ishimoto, G. Christou, and D. N. Hendrickson, *Inorg. Chem.*, **40**, 4604 (2001). d) C. Boskovic, E. K. Brechin, W. E. Streib, K. Folting, D. N. Hendrickson, and G. Christou, *J. Am. Chem. Soc.*, **124**, 3725 (2002). e) E. K. Brechin, C. Boskovic, W. Wernsdorfer, J. Yoo,

A. Yamaguchi, E. C. Sanudo, T. Concolino, A. L. Rheingold, H. Ishimoto, D. N. Hendrickson, and G. Christou, *J. Am. Chem. Soc.*, **124**, 9710 (2002). f) E. K. Brechin, M. Soler, J. Davidson, D. N. Hendrickson, S. Parsons, and G. Christou, *Chem. Commun.*, **2002**, 2252. g) C. Boskovic, R. Bircher, P. L. W. Tregenna-Piggott, H. U. Güdel, C. Paulsen, W. Wernsdorfer, A.-L. Barra, E. Khatsko, A. Neels, and H. Stoeckli-Evans, *J. Am. Chem. Soc.*, **125**, 14046 (2003). h) A. J. Tasiopoulos, A. Vinslava, W. Wernsdorfer, K. A. Abboud, and G. Christou, *Angew. Chem., Int. Ed.*, **43**, 2117 (2004). i) M. Murugesu, M. Habrych, W. Wernsdorfer, K. A. Abboud, and G. Christou, *J. Am. Chem. Soc.*, **126**, 4766 (2004). j) M. Soler, W. Wernsdorfer, K. Folting, M. Pink, and G. Christou, *J. Am. Chem. Soc.*, **126**, 2156 (2004). k) M. Murugesu, J. Raftery, W. Wernsdorfer, G. Christou, and E. K. Brechin, *Inorg. Chem.*, **43**, 4203 (2004). l) E. C. Sanudo, W. Wernsdorfer, K. A. Abboud, and G. Christou, *Inorg. Chem.*, **43**, 4137 (2004). m) L. M. Wittick, K. S. Murray, B. Moubaraki, S. R. Batten, L. Spiccia, and K. Berry, *J. Chem. Soc., Dalton Trans.*, **2004**, 1003. n) N. Aliaga-Alcalde, R. S. Edwards, S. O. Hill, W. Wernsdorfer, K. Folting, and G. Christou, *J. Am. Chem. Soc.*, **126**, 12503 (2004). o) P. King, W. Wernsdorfer, K. A. Abboud, and G. Christou, *Inorg. Chem.*, **43**, 7315 (2004). p) G. Rajaraman, M. Murugesu, E. C. Sañudo, M. Soler, W. Wernsdorfer, M. Helliwell, C. Muryn, J. Raftery, S. J. Teat, G. Christou, and E. K. Brechin, *J. Am. Chem. Soc.*, **126**, 15445 (2004).

14 H. Miyasaka, R. Clérac, W. Wernsdorfer, L. Lecren, C. Bonhomme, K. Sugiura, and M. Yamashita, *Angew. Chem., Int. Ed.*, **43**, 2801 (2004).

15 a) C. Delfs, D. Gatteschi, L. Pardi, R. Sessoli, K. Wieghardt, and D. Hanke, *Inorg. Chem.*, **32**, 3099 (1993). b) A. L. Barra, A. Caneschi, A. Cornia, F. Fabrizi de Biani, D. Gatteschi, C. Sangregorio, R. Sessoli, and L. Sorace, *J. Am. Chem. Soc.*, **121**, 5302 (1999). c) D. Gatteschi, R. Sessoli, and A. Cornia, *Chem. Commun.*, **2000**, 725. d) H. Oshio, N. Hoshino, and T. Ito, *J. Am. Chem. Soc.*, **122**, 12602 (2000). e) C. Benelli, J. Cano, Y. Journaux, R. Sessoli, G. A. Solan, and R. E. P. Winpenny, *Inorg. Chem.*, **40**, 188 (2001). f) J. C. Goodwin, R. Sessoli, D. Gatteschi, W. Wernsdorfer, A. K. Powell, and S. L. Heath, *J. Chem. Soc., Dalton Trans.*, **2000**, 1835. g) H. Oshio, N. Hoshino, T. Ito, and M. Nakano, *J. Am. Chem. Soc.*, **126**, 8805 (2004).

16 a) C. Cadiou, M. Murrie, C. Paulsen, V. Villar, W. Wernsdorfer, and R. E. P. Winpenny, *Chem. Commun.*, **2001**, 2666. b) H. Andres, R. Basler, A. J. Blake, C. Cadiou, G. Chaboussant, C. M. Grant, H.-U. Güdel, M. Murrie, S. Parsons, C. Paulsen, F. Semadini, V. Villar, W. Wernsdorfer, and R. E. P. Winpenny, *Chem.—Eur. J.*, **8**, 4867 (2002). c) E.-C. Yang, W. Wernsdorfer, S. Hill, R. S. Edwards, M. Nakano, S. Maccagnano, L. N. Zakharov, A. L. Rheingold, G. Christou, and D. N. Hendrickson, *Polyhedron*, **22**, 1727 (2003). d) M. Moragues-Cánovas, M. Helliwell, L. Ricard, E. Rivière, W. Wernsdorfer, E. Brechin, and T. Mallah, *Eur. J. Inorg. Chem.*, **2004**, 2219.

17 S. L. Castro, Z. Sun, C. M. Grant, J. C. Bollinger, D. N. Hendrickson, and G. Christou, *J. Am. Chem. Soc.*, **120**, 2365 (1998).

18 E. Yang, D. N. Hendrickson, W. Wernsdorfer, M. Nakano, L. N. Zakharov, R. D. Sommer, A. L. Rheingold, M. Ledezma-Gairaud, and G. Christou, *J. Appl. Phys.*, **91**, 7382 (2002).

19 a) A. R. Schake, H.-L. Tsai, R. J. Webb, K. Folting, G. Christou, and D. N. Hendrickson, *Inorg. Chem.*, **33**, 6020 (1994). b) J. J. Sokol, A. G. Hee, and J. R. Long, *J. Am. Chem. Soc.*, **124**, 7656 (2002). c) S. Karasawa, G. Zhou, H. Morikawa, and N. Koga, *J. Am. Chem. Soc.*, **125**, 13676 (2003). d) H. J. Choi, J. J. Sokol, and J. R. Long, *Inorg. Chem.*, **43**, 1606 (2004). e) S. Osa, T. Kido, N. Matsumoto, N. Re, A. Pochaba, and J. Mrozinski, *J. Am. Chem. Soc.*, **126**, 420 (2004). f) C. M. Zaleski, E. C. Depperman, J. W. Kampf, M. L. Kirk, and V. L. Pecoraro, *Angew. Chem., Int. Ed.*, **43**, 3912 (2004). g) E. J. Schelter, A. V. Prosvirin, and K. R. Dunbar, *J. Am. Chem. Soc.*, **126**, 15004 (2004). h) A. Mishra, W. Wernsdorfer, K. A. Abboud, and G. Christou, *J. Am. Chem. Soc.*, **126**, 15648 (2004). i) H. Oshio, M. Nihei, A. Yoshida, H. Nojiri, M. Nakano, A. Yamaguchi, Y. Karaki, and H. Ishimoto, *Chem.—Eur. J.*, **11**, 843 (2005).

20 H. Miyasaka, T. Nezu, K. Sugimoto, K. Sugiura, M. Yamashita, and R. Clérac, *Chem.—Eur. J.*, in press.

21 J. R. Friedman, M. P. Sarachik, J. Tejada, J. Maciejewski, and R. Ziolo, *J. Appl. Phys.*, **79**, 6031 (1996).

22 J. R. Friedman, M. P. Sarachik, J. Tejada, and R. Ziolo, *Phys. Rev. Lett.*, **76**, 3830 (1996).

23 L. Thomas, F. Lionti, R. Ballou, D. Gatteschi, R. Sessoli, and B. Barbara, *Nature*, **383**, 145 (1996).

24 E. M. Chudnovsky, *Science*, **274**, 938 (1996).

25 J. R. Friedman, M. P. Sarachik, J. M. Hernandez, X. X. Zhang, J. Tejada, E. Molins, and R. Ziolo, *J. Appl. Phys.*, **81**, 3978 (1997).

26 A.-L. Barra, L.-C. Brunel, D. Gatteschi, L. Pardi, and R. Sessoli, *Acc. Chem. Res.*, **31**, 460 (1998).

27 W. Wernsdorfer, N. Aliaga-Alcalde, D. N. Hendrickson, and G. Christou, *Nature*, **416**, 406 (2002).

28 W. Wernsdorfer, S. Bhaduri, R. Tiron, D. N. Hendrickson, and G. Christou, *Phys. Rev. Lett.*, **89**, 197201 (2002).

29 R. Tiron, W. Wernsdorfer, N. Aliaga-Alcalde, and G. Christou, *Phys. Rev. B*, **68**, 140407 (2003).

30 K. Park, M. R. Pederson, S. L. Richardson, N. Aliaga-Alcalde, and G. Christou, *Phys. Rev. B*, **68**, 020405 (2003).

31 S. Hill, R. S. Edwards, N. Aliaga-Alcalde, and G. Christou, *Science*, **302**, 1015 (2003).

32 E. del Barco, A. D. Kent, E. M. Rumberger, D. N. Hendrickson, and G. Christou, *Phys. Rev. Lett.*, **91**, 047203 (2003).

33 R. S. Edwards, S. Maccagnano, E.-C. Yang, S. Hill, W. Wernsdorfer, D. N. Hendrickson, and G. Christou, *J. Appl. Phys.*, **93**, 7807 (2003).

34 L. Sorace, W. Wernsdorfer, C. Thirion, A.-L. Barra, M. Pacchioni, D. Mailly, and B. Barbara, *Phys. Rev. B*, **68**, 220407 (2003).

35 R. Tiron, W. Wernsdorfer, D. Foguet-Albiol, N. Aliaga-Alcalde, and G. Christou, *Phys. Rev. Lett.*, **91**, 227203 (2003).

36 R. J. Glauber, *J. Math. Phys.*, **4**, 294 (1963).

37 M. Susuki and R. Kubo, *J. Phys. Soc. Jpn.*, **24**, 51 (1968).

38 L. Onsager, *Phys. Rev.*, **65**, 117 (1944).

39 In Ref. 36, the energy barrier $\Delta_{\mathrm{Glauber}}$ is equal to $4J$ based on the following Hamiltonian: $H = -J\sum_i \sigma_i\sigma_{i+1}$ with $\sigma_i = \pm 1$. In this paper, we have used: $H = -2J\sum_i S_{\mathrm{T}zj}S_{\mathrm{T}z(i+1)}$ which is equivalent with the Glauber's notation to $H = -2JS_{\mathrm{T}}^2\sum_i \sigma_i\sigma_{i+1}$. Therefore with this Hamiltonian definition, the energy gap $\Delta_{\mathrm{Glauber}}$ is $8JS_{\mathrm{T}}{}^2$.

40 a) A. Caneschi, D. Gatteschi, N. Lalioti, R. Sessoli, G. Venturi, A. Vindigni, A. Rettori, M. G. Pini, and M. A. Novak, *Angew. Chem., Int. Ed.*, **40**, 1760 (2001). b) A. Caneschi, D. Gatteschi, N. Lalioti, R. Sessoli, L. Sorace, V. Tangoulis, and A. Vindigni, *Chem.—Eur. J.*, **8**, 286 (2002). c) A. Caneschi, D. Gatteschi, N. Lalioti, C. Sangregorio, R. Sessoli, G. Venturi, A. Vindigni, A. Rettori, M. G. Pini, and M. A. Novak, *Europhys.*

Lett., **58**, 771 (2002).

41 L. Bogani, A. Caneschi, M. Fedi, D. Gatteschi, M. Massi, M. A. Novak, M. G. Pini, A. Rettori, R. Sessoli, and A. Vindigni, *Phys. Rev. Lett.*, **92**, 207204 (2004).

42 R. Clérac, H. Miyasaka, M. Yamashita, and C. Coulon, *J. Am. Chem. Soc.*, **124**, 12837 (2002).

43 a) S. Wang, J.-L. Zuo, S. Gao, Y. Song, H.-C. Zhou, Y.-Z. Zhang, and X.-Z. You, *J. Am. Chem. Soc.*, **126**, 8900 (2004). b) N. Shaikh, A. Panja, S. Goswami, P. Banerjee, P. Vojtísek, Y.-Z. Zhang, G. Su, and S. Gao, *Inorg. Chem.*, **43**, 849 (2004). c) J.-P. Costes, J. M. Clemente-Juan, F. Dahan, and J. Milon, *Inorg. Chem.*, **43**, 8200 (2004). d) N. E. Chakov, W. Wernsdorfer, K. A. Abboud, and G. Christou, *Inorg. Chem.*, **43**, 5919 (2004).

44 a) R. Lescouëzec, J. Vaissermann, C. Ruiz-Pérez, F. Lloret, R. Carrasco, M. Julve, M. Verdaguer, Y. Dromzée, D. Gatteschi, and W. Wernsdorfer, *Angew. Chem., Int. Ed.*, **42**, 1483 (2003). b) F. Chang, S. Gao, H.-L. Sun, Y.-L. Hou, and G. Su, Proceeding of the ICSM 2002 Conference, Shanghai, China. c) L. M. Toma, R. Lescouëzec, F. Lloret, M. Julve, J. Vaissermann, and M. Verdaguer, *Chem. Commun.*, **2003**, 1850.

45 T.-F. Liu, D. Fu, S. Gao, Y.-Z. Zhang, H.-L. Sun, G. Su, and Y.-J. Liu, *J. Am. Chem. Soc.*, **125**, 13976 (2003).

46 E. Pardo, R. Ruiz-García, F. Lloret, J. Faus, M. Julve, Y. Journaux, F. Delgado, and C. Ruiz-Pérez, *Adv. Mater.*, **16**, 1597 (2004).

47 B. J. Kennedy and K. S. Murray, *Inorg. Chem.*, **24**, 1552 (1985).

48 a) H. Miyasaka, N. Matsumoto, H. Okawa, N. Re, E. Gallo, and C. Floriani, *Angew. Chem., Int. Ed.*, **34**, 1446 (1995). b) H. Miyasaka, N. Matsumoto, H. Okawa, N. Re, E. Gallo, and C. Floriani, *J. Am. Chem. Soc.*, **118**, 981 (1996). c) N. Re, E. Gallo, C. Floriani, H. Miyasaka, and N. Matsumoto, *Inorg. Chem.*, **35**, 5964 (1996). d) N. Re, E. Gallo, C. Floriani, H. Miyasaka, and N. Matsumoto, *Inorg. Chem.*, **35**, 6004 (1996). e) H. Miyasaka, N. Matsumoto, N. Re, E. Gallo, and C. Floriani, *Inorg. Chem.*, **36**, 670 (1997). f) H. Miyasaka, H. Ieda, N. Matsumoto, N. Re, R. Crescenzi, and C. Floriani, *Inorg. Chem.*, **37**, 255 (1998). g) H. Miyasaka, H. Okawa, A. Miyazaki, and T. Enoki, *J. Chem. Soc., Dalton Trans.*, **1998**, 3991. h) H. Miyasaka, H. Okawa, A. Miyazaki, and T. Enoki, *Inorg. Chem.*, **37**, 4878 (1998). i) H. Miyasaka, H. Okawa, and N. Matsumoto, *Mol. Cryst. Liq. Cryst.*, **335**, 303 (1999). j) H. Miyasaka, H. Ieda, N. Matsumoto, K. Sugiura, and M. Yamashita, *Inorg. Chem.*, **42**, 3509 (2003). k) M. Clemente-León, E. Coronado, J. R. Galán-Mascarós, C. J. Gómez-García, T. Woike, and J. M. Clemente-Juan, *Inorg. Chem.*, **40**, 87 (2001). l) P. Przychodzén, K. Lewinski, M. Balanda, R. Pelka, M. Rams, T. Wasiutynski, C. Guyard-Duhayon, and B. Sieklucka, *Inorg. Chem.*, **43**, 2967 (2004).

49 N. Matsumoto, Y. Sunatsuki, H. Miyasaka, Y. Hashimoto, D. Luneau, and J.-P. Tuchagues, *Angew. Chem., Int. Ed.*, **38**, 171 (1999).

50 a) P. Chaudhuri, M. Winter, B. P. C. Della Védova, E. Bill, A. Trautwein, S. Gehring, P. Fleischhauer, B. Nuber, and J. Weiss, *Inorg. Chem.*, **30**, 2148 (1991). b) P. Chaudhuri, M. Winter, B. P. C. Della Védova, P. Fleischhauer, W. Haase, U. Flörke, and H. Haupt, *Inorg. Chem.*, **30**, 4777 (1991). c) F. Birkelbach, M. Winter, U. Flörke, H. Haupt, C. Butzlaff, M. Lengen, E. Bill, A. X. Trautwein, K. Wieghardt, and P. Chaudhuri, *Inorg. Chem.*, **33**, 3990 (1994). d) F. Birkelbach, T. Weyhermüller, M. Lengen, M. Gerdan, A. X. Trautwein, K. Wieghardt, and P. Chaudhuri, *J. Chem. Soc., Dalton Trans.*, **1997**, 4529. e) D. Burdinski, F. Birkelbach, T. Weyhermüller, U. Flörke, H. Haupt, M. Lengen, A. X. Trautwein, E. Bill, K. Wieghardt, and P. Chaudhuri, *Inorg. Chem.*, **37**, 1009 (1998). f) F. Birkelbach, U. Flörke, H. Haupt, C. Butzlaff, A. X. Trautwein, K. Wieghardt, and P. Chaudhuri, *Inorg. Chem.*, **37**, 2000 (1998). g) H. Miyasaka, T. Nezu, F. Iwahori, S. Furukawa, K. Sugimoto, R. Clérac, K. Sugiura, and M. Yamashita, *Inorg. Chem.*, **42**, 4501 (2003).

51 H. Miyasaka, K. Mizushima, K. Sugiura, and M. Yamashita, *Synth. Met.*, **137**, 1245 (2003).

52 H. Miyasaka, S. Furukawa, S. Yanagida, K. Sugiura, and M. Yamashita, *Inorg. Chim. Acta*, **357**, 1619 (2004).

53 H. Miyasaka, T. Nezu, K. Sugimoto, K. Sugiura, M. Yamashita, and R. Clérac, *Inorg. Chem.*, **43**, 5486 (2004).

54 H. Miyasaka, R. Clérac, K. Mizushima, K. Sugiura, M. Yamashita, W. Wernsdorfer, and C. Coulon, *Inorg. Chem.*, **42**, 8203 (2003).

55 C. Coulon, R. Clérac, L. Lecren, W. Wernsdorfer, and H. Miyasaka, *Phys. Rev. B*, **69**, 132408 (2004).

56 In solution, Mn^{III} salen-type Schiff-base complexes are in equilibrium between the monomeric species $[Mn(SB)(S)_2]^+$ and the dimeric species $[Mn_2(SB)_2(S)_2]^{2+}$ (SB = salen-type Schiff-base ligand, S = monodentate solvent ligand). The crystalline solid-state-form depends on the steric characteristics of the salen-type Schiff-base ligand, the used solvent, and donor-activity of coordinating species (solvent or other ligand).

57 H. J. Gerritsen and E. S. Sabinsky, *Phys. Rev.*, **132**, 1507 (1963).

58 H. Miyasaka, R. Clérac, T. Ishii, H.-C. Chang, S. Kitagawa, and M. Yamashita, *J. Chem. Soc., Dalton Trans.*, **2002**, 1528.

59 Y. Sato, H. Miyasaka, N. Matsumoto, and H. Okawa, *Inorg. Chim. Acta*, **247**, 57 (1996).

60 Y. Cringh, S. W. Gordon-Wylie, R. E. Norman, G. R. Clark, S. T. Weintraub, and C. P. Horwitz, *Inorg. Chem.*, **36**, 4968 (1997).

61 C. E. Hulme, M. Watkinson, M. Haynes, R. G. Pritchard, C. A. McAuliffe, N. Jaiboon, B. Beagley, A. Sousa, M. R. Bermejo, and M. Fondo, *J. Chem. Soc., Dalton Trans.*, **1997**, 1805.

62 N. Matsumoto, Z. J. Zhong, H. Okawa, and S. Kida, *Inorg. Chim. Acta*, **160**, 153 (1989).

63 N. Matsumoto, N. Takemoto, A. Ohyosi, and H. Okawa, *Bull. Chem. Soc. Jpn.*, **61**, 2984 (1988).

64 M. R. Bermejo, A. Castiñeiras, J. C. Garcia-Monteagudo, M. Rey, A. Sousa, M. Watkinson, C. A. McAuliffe, R. G. Pritchard, and R. L. Beddoes, *J. Chem. Soc., Dalton Trans.*, **1996**, 2935.

65 A. Garcia-Deibe, A. Sousa, M. R. Bermejo, P. P. MacRory, C. A. McAuliffe, R. G. Pritchard, and M. Hellowell, *J. Chem. Soc., Chem. Commun.*, **1991**, 728.

66 a) M. Mikuriya, Y. Yamato, and T. Tokii, *Bull. Chem. Soc. Jpn.*, **65**, 1466 (1992). b) H. Li, Z. J. Zhong, C. Duan, X. You, T. C. W. Mak, and B. Wu, *J. Coord. Chem.*, **41**, 183 (1997).

67 N. Matsumoto, H. Okawa, S. Kida, T. Ogawa, and A. Ohyoshi, *Bull. Chem. Soc. Jpn.*, **62**, 3812 (1989).

68 H.-L. Shyu, H.-H. Wei, and Y. Wang, *Inorg. Chim. Acta*, **290**, 8 (1999).

69 M. Corbella, R. Costa, J. Ribas, P. H. Fries, J.-M. Latour, L. Öhrström, X. Solans, and V. Rodrigez, *Inorg. Chem.*, **35**, 1857 (1996).

70 R. A. Krause and D. H. Busch, *J. Am. Chem. Soc.*, **82**, 4830 (1960).

71 As far as we are aware, there is indeed one example of

quasi-1D compound in the literature with oximato-bridge that has been reported, nevertheless without X-ray diffraction structural analysis: F. Lloret, R. Ruiz, B. Cervera, I. Castro, M. Julve, J. Faus, J. A. Real, F. Sapiña, Y. Journaux, J. C. Colin, and M. Verdaguer, *J. Chem. Soc., Chem. Commun.*, **1994**, 2615.

72 C. J. O'Connor, *Prog. Inorg. Chem.*, **29**, 203 (1982).

73 Inter-chain magnetic interactions (J''), probably mediated by weak π overlaps of aromatic rings, are most likely antiferromagnetic.

74 The weak anisotropy which appears below 20 K in the plane perpendicular to the chains may be the consequence of a misorientation of the crystals.

75 Strictly speaking this approximation is valid for $D < 0$ and $k_B T \ll -5D$ which is a reasonable treatment in our system below 15 K.

76 C. J. Thompson, "Phase Transition and Critical Phenomena," ed by C. Domb and M. S. Green, Academic Press, London (1972), Vol. 1, pp. 177–226.

77 W. Wernsdorfer, *Adv. Chem. Phys.*, **118**, 99 (2001).

78 a) R. V. Chamberlin, G. Mozurkewich, and R. Orbach, *Phys. Rev. Lett.*, **52**, 867 (1984). b) C. De Dominics, H. Orland, and F. Lainée, *J. Phys., Lett.*, **46**, L-463 (1985). c) G. H. Weiss, M. Dishon, A. M. Long, J. T. Bendler, A. A. Jones, P. T. Inglefield, and A. Bandis, *Polymer*, **35**, 1880 (1994).

79 A. H. Morrish, "The Physical Principles of Magnetism," Wiley, New York (1965); C. Bean and J. D. Livingston, *J. Appl. Phys.*, **30**, 120S (1959).

80 J. A. Mydosh, "Spin Glasses: An Experimental Introduction," Taylor & Francis, London (1993).

81 K. Moorjani and J. M. Coey, "Magnetic Glasses," Elsevier, New York (1984).

82 D. Chowdhury, "Spin Glasses and Other Frustrated Systems," Princeton University Press, New Jersey (1986).

83 K. Binder and A. P. Young, *Rev. Mod. Phys.*, **58**, 801 (1986).

84 Considering the following Hamiltonian: $H = -2J' \sum_i S_{Tzi} S_{Tz(i+1)}$ which is equivalent to the Glauber's notation: $H = -2J' S_T^2 \sum_i \sigma_{zi} \sigma_{z(i+1)}$ with $\sigma_i = \pm 1$.

85 J. M. Loveluck, S. W. Lovesey, and S. J. Aubry, *J. Phys. C: Solid State Phys.*, **8**, 3841 (1975).

86 In this case, the domain walls are localized on one unit cell: B. Barbara, *J. Magn. Magn. Mater.*, **129**, 79 (1994). For smaller values of D/J, the Bloch walls are broader and the gap is a function of D and J.

87 C. Sangregorio, T. Ohm, C. Paulsen, R. Sessoli, and D. Gatteschi, *Phys. Rev. Lett.*, **78**, 4645 (1997).

88 D. N. Hendrickson, G. Christou, I. Hidehiko, J. Yoo, E. K. Brechin, A. Yamaguchi, E. M. Rumberger, S. M. J. Aubin, Z. Sun, and G. Aromi, *Polyhedron*, **20**, 1479 (2001).

89 a) J. K. Leal da Silva, A. G. Moreira, M. S. Soares, and F. C. S. Barreto, *Phys. Rev. E*, **52**, 4527 (1995). b) J. H. Luscombe, M. Luban, and J. P. Reynolds, *Phys. Rev. E*, **53**, 5852 (1996).

90 This result is true for any value of D as long as the spins are considered as classical.

91 The obtained value of J_{AF} may be over estimated as antiferromagnetic inter-chain coupling may also be present. However this coupling should remain very weak, i.e. negligible, as no magnetic phase transition has been observed above 40 mK.

92 H. Miyasaka, K. Nakata, K. Sugiura, M. Yamashita, and R. Clérac, *Angew. Chem., Int. Ed.*, **43**, 707 (2004).

93 A. Maignan, V. Hardy, S. Hébert, M. Drillon, M. R. Lees, O. Petrenko, D. M. K. Paul, and D. Khomskii, *J. Chem. Mater.*, **14**, 1231 (2004).

94 C. Coulon, R. Clérac, W. Wernsdorfer, and H. Miyasaka, unpublished results.

Award recipient

Hitoshi Miyasaka was born in Matsumoto, Nagano in 1969. He received his B.S. (1992) from Shimane University, and then his M.S. (1994) and Ph.D. (1997) from Kyushu University on a research subject of molecule-based magnetic materials of cyano-bridged Mn^{III} salen-type compounds under the supervision of Prof. H. Okawa and Prof. N. Matsumoto. Then, he joined the group of Prof. S. Kitagawa at Kyoto University as a postdoctoral researcher of JSPS (1998–2000) and started a study of functional materials based on metal–metal bonded compounds. During one year from the end of 1999, he was a postdoctoral researcher at the group of Prof. K. R. Dunbar at Texas A&M University (College Station, Texas, U. S. A.) and expanded the chemistry of low-dimensional network compounds based on Ru–Ru compounds and poly-cyano organic groups. At this time, he started to work with Dr. R. Clérac who was also a postdoctoral researcher of Dunbar's group. Since October in 2000, he has been an assistant professor at the Graduate School of Science, Tokyo Metropolitan University (Prof. M. Yamashita's group). He has also been a research member of PRESTO project ("Structural Ordering and Physical Properties") of Japan Science and Technology Agency (JST) in 2002–2004. His current research interests are molecular materials involved in unique electronic systems or magnetic systems such as Single-Chain Magnets and SMM-based network compounds. He received the Chemical Society of Japan Award for Young Chemists for 2003.

Rodolphe Clérac born in 1971 in Versailles (France), received his education at the University of Bordeaux 1, France. His Ph.D. work was devoted to the physical properties of molecular antiferromagnetic materials under the supervision of Prof. C. Coulon (in 1997). After short postdoctoral stay in the group of Prof. O. Kahn (ICMCB, Bordeaux), he joined in 1998 Prof. K. R. Dunbar's group at Michigan State University (East Lansing, Michigan, U. S. A.) and worked on the magnetic properties of coordination chemistry based materials. In 1999, he moved with Prof. K. R. Dunbar's group to Texas A&M University (College Station, Texas, U. S. A.) where he collaborated with Prof. F. A. Cotton on the magnetic properties of metal–metal bonded complexes. He joined the University of Bordeaux 1 in 2000, as "Maître de Conférence" (associate professor). Since 2000, Dr. R. Clérac has developed at the Centre de Recherche Paul Pascal (CNRS) a new research team interested in the synthesis and physical studies of "molecular magnetic materials." In this research field, he has published ca. 110 articles. The main subjects currently developed in his group deal on hybrid magnetic materials (liquid crystals, gels, and nano-composites), molecule-based magnets (including Single-Molecule magnets and Single-Chain magnets) and fullerene salts.